Chapter 5

CONSTRUCTION OF FINITE ELEMENT SUBSPACES

5.1 Introduction

The finite element method provides a general procedure for the construction of admissible spaces $\mathcal{U}_h$ and, if necessary, $\mathcal{W}_h$, in connection with the weighted-residual and variational methods discussed in the previous two chapters.

By way of background, define the *support* of a real-valued function $f(\mathbf{x})$ in its domain $\Omega \subset \mathbb{R}^n$ as the closure of the set of all points $\mathbf{x}$ in the domain for which $f(\mathbf{x}) \neq 0$, namely

$$\operatorname{supp} f \;=\; \overline{\{\mathbf{x} \in \Omega \;\mid\; f(\mathbf{x}) \neq 0\}}\,. \tag{5.1}$$

With reference to the general form of the approximation functions u_h and w_h given by equations (3.24), respectively, one may establish a distinction between *global* and *local* approximation methods. Local approximation methods are those for which $\operatorname{supp} \varphi_I$ is "small" compared to the size of the domain of approximation, whereas global methods employ interpolation functions with relatively "large" support.

Global and local approximation methods present both advantages and disadvantages. Global methods are often capable of providing excellent estimates of a solution with relatively small computational effort, especially when the analyst has a good understanding of the expected solution characteristics. However, a proper choice of global interpolation functions may not always be readily available, as in the case of complicated domains, where satisfaction of any boundary conditions could be a difficult, if not an insurmountable task. In addition,

global methods rarely lend themselves to a straightforward algorithmic implementation, and even when they do, they almost invariably yield dense linear systems of the form (3.30), which may require substantial computational effort to solve.

Local methods are more suitable for algorithmic implementation than global methods, as they can easily satisfy Dirichlet (or essential) boundary conditions, and they typically yield "banded" linear algebraic systems. Moreover, these methods are flexible in allowing local refinements in the approximation, when warranted by the analysis. However, local methods can be surprisingly expensive, even for simple problems, when the desired degree of accuracy is high. The so-called *global-local* approximation methods combine both global and local interpolation functions in order to exploit the positive characteristics of both methods.

Interpolation functions that appear in equations (3.24) need to satisfy certain general admissibility criteria. These criteria are motivated by the requirement that the resulting finite-dimensional solution spaces be well-defined and capable of accurately and uniformly approximating the exact solutions. In particular, all families of interpolation functions $\{\varphi_1, \ldots, \varphi_N\}$ should have the following properties:

(a) For any $\mathbf{x} \in \Omega$, there exists an I with $1 \leq I \leq N$, such that $\varphi_I(\mathbf{x}) \neq 0$. In other words, the interpolation functions should "cover" the whole domain of analysis. Indeed, if the above property is not satisfied, it follows that there exist interior points of Ω where the exact solution is not at all approximated.

(b) All interpolation functions should satisfy the Dirichlet (or essential) boundary conditions, if required by the underlying weak form, as discussed in Chapters 3 and 4.

(c) The interpolation functions should be *linearly independent* in the domain of analysis. To further elaborate on this point, let $\mathcal{U}_h$ be the space of admissible solutions spanned by functions $\{\varphi_1, \ldots, \varphi_N\}$, namely

$$\mathcal{U}_h \;=\; \{u_h \quad | \quad u_h \;=\; \sum_{I=1}^{N} \alpha_I \, \varphi_I \quad , \quad \alpha_I \in \mathbb{R},\; I = 1, \ldots, N\} \; . \tag{5.2}$$

Linear independence of the interpolation functions is equivalent to stating that

$$\sum_{I=1}^{N} \alpha_I \, \varphi_I \;=\; 0 \quad \Leftrightarrow \quad \alpha_I \;=\; 0 \quad , \quad I = 1, \ldots, N \; . \tag{5.3}$$

An alternative statement of linear independence of functions $\{\varphi_1, \ldots, \varphi_N\}$ is that

given any $u_h \in \mathcal{U}_h$, there exists a unique set of parameters $\{\alpha_1, \ldots, \alpha_N\}$, such that

$$u_h \;=\; \sum_{I=1}^{N} \alpha_I \, \varphi_I \;. \tag{5.4}$$

If property (c) holds, then functions $\{\varphi_1, \ldots, \varphi_N\}$ are said to form a *basis* of $\mathcal{U}_h$. Linear independence of the interpolation functions is essential for the derivation of approximate solutions. Indeed, if parameters $\{\alpha_1, \ldots, \alpha_N\}$ are not uniquely defined for any given $u_h \in \mathcal{U}_h$, then the linear algebraic system (3.30) does not possess a unique solution and, consequently, the discrete problem is ill-posed.

(d) Interpolation functions must satisfy the integrability requirements emanating from the associated weak forms, as discussed in Chapters 3 and 4.

(e) The family of interpolation functions should possess sufficient "approximating power". One of the most important features of Hilbert spaces is that they provide a suitable framework for examining the issue of how (and in what sense) a function $u_h \in \mathcal{U}_h \subset \mathcal{U}$, defined as

$$u_h \;=\; \sum_{I=1}^{N} \alpha_I \, \varphi_I \tag{5.5}$$

approximates a function $u \in \mathcal{U}$ as N increases. In order to address the above point, consider a set of functions $\{\varphi_1, \varphi_2, \ldots, \varphi_N, \ldots\}$, which are linearly independent in $\mathcal{U}$ and, thus, form a countably infinite basis.[1] These functions are termed *orthonormal* in $\mathcal{U}$ if

$$< \varphi_I, \varphi_J > \;=\; \begin{cases} 1 & \text{if } I = J \\ 0 & \text{if } I \neq J \end{cases} \;. \tag{5.6}$$

Any countably infinite basis can be orthonormalized by means of a *Gram-Schmidt orthogonalization* procedure, as follows: starting with the first function φ_1, let

$$\psi_1 \;=\; \frac{\varphi_1}{\|\varphi_1\|} \,, \tag{5.7}$$

so that, clearly,

$$< \psi_1, \psi_1 > \;=\; \|\psi_1\|^2 \;=\; 1 \;. \tag{5.8}$$

Then, let

$$\psi_2 \;=\; a_2[\varphi_2 - \; < \varphi_2, \psi_1 > \psi_1] \;, \tag{5.9}$$

[1] Hilbert spaces can be shown to always possess such a basis.

where a_2 is a scalar parameter to be determined. It is immediately seen from (5.9) that

$$\begin{aligned} < \psi_1, \psi_2 > &= < \psi_1, a_2\varphi_2 \; - \; a_2 < \varphi_2, \psi_1 > \psi_1 > \\ &= a_2 < \psi_1, \varphi_2 > \; - \; a_2 < \psi_1, \psi_1 >< \psi_1, \varphi_2 > = \; 0 \; . \end{aligned} \tag{5.10}$$

The scalar parameter a_2 is determined so that $\|\psi_2\| = 1$, namely

$$a_2 \; = \; \frac{1}{\|\varphi_2 \; - \; < \varphi_2, \psi_1 > \psi_1\|} \; . \tag{5.11}$$

In general, the function φ_{K+1}, $K = 1, 2, \ldots$, gives rise to ψ_{K+1} defined as

$$\psi_{K+1} \; = \; a_{K+1}[\varphi_{K+1} \; - \; \sum_{I=1}^{K} < \varphi_{K+1}, \psi_I > \psi_I] \; , \tag{5.12}$$

where

$$a_{K+1} \; = \; \frac{1}{\|\varphi_{K+1} \; - \; \sum_{I=1}^{K} < \varphi_{K+1}, \psi_I > \psi_I\|} \; . \tag{5.13}$$

To establish that $\{\psi_1, \psi_2, \ldots, \psi_N, \ldots\}$ are orthonormal, it suffices to show by induction that if $\{\psi_1, \psi_2, \ldots, \psi_K\}$ are orthonormal, then ψ_{K+1} is orthonormal with respect to each of the first K members of the sequence. Indeed, using (5.12) it is seen that

$$\begin{aligned} < \psi_{K+1}, \psi_K > &= < a_{K+1}\varphi_{K+1} \; - \; a_{K+1} \sum_{I=1}^{K} < \varphi_{K+1}, \psi_I > \psi_I, \psi_K > \\ &= < a_{K+1}\varphi_{K+1}, \psi_K > \; - \; \sum_{I=1}^{K-1} a_{K+1} < \varphi_{K+1}, \psi_I >< \psi_I, \psi_K > \\ &\quad - a_{K+1} < \varphi_{K+1}, \psi_K >< \psi_K, \psi_K > = \; 0 \end{aligned} \tag{5.14}$$

and, for $N < K$,

$$\begin{aligned} < \psi_{K+1}, \psi_N > &= < a_{K+1}\varphi_{K+1} \; - \; a_{K+1} \sum_{I=1}^{K} < \varphi_{K+1}, \psi_I > \psi_I, \psi_N > \\ &= < a_{K+1}\varphi_{K+1}, \psi_N > \; - \; \sum_{I=1}^{N-1} a_{K+1} < \varphi_{K+1}, \psi_I >< \psi_I, \psi_N > \\ &\quad - \sum_{I=N+1}^{K} a_{K+1} < \varphi_{K+1}, \psi_I >< \psi_I, \psi_N > \\ &\quad - a_{K+1} < \varphi_{K+1}, \psi_N >< \psi_N, \psi_N > = \; 0 \; , \end{aligned} \tag{5.15}$$

which establishes the desired result.

Since $\{\psi_1, \psi_2, \ldots, \psi_N, \ldots\}$ is an orthonormal basis in $\mathcal{U}$, one may uniquely write any $u \in \mathcal{U}$ in the form

$$u \;=\; \sum_{I=1}^{\infty} \alpha_I \, \psi_I \;, \tag{5.16}$$

which may be interpreted as meaning that given any $\epsilon > 0$, there exists a positive integer N and scalars α_I, such that

$$\| u \;-\; \sum_{I=1}^{n} \alpha_I \, \psi_I \| \;<\; \epsilon \;, \tag{5.17}$$

for all $n > N$. The coefficients α_I in (5.16) are known as the *Fourier coefficients* of u with respect to the given basis and can be easily determined by exploiting the orthonormality of ψ_I and noting that

$$\begin{aligned} < u, \psi_J > \;&=\; < \sum_{I=1}^{\infty} \alpha_I \, \psi_I, \psi_J > \\ &= \sum_{I=1}^{\infty} \alpha_I < \psi_I, \psi_J > \;=\; \alpha_J \;. \end{aligned} \tag{5.18}$$

Therefore, one obtains the *Fourier representation* of u with respect to the given orthonormal basis as

$$u \;=\; \sum_{I=1}^{\infty} < u, \psi_I > \psi_I \;. \tag{5.19}$$

It is noted that the natural norm of u satisfies *Parseval's identity*, namely,

$$\| u \|^2 \;=\; \sum_{I=1}^{\infty} \mid \alpha_I \mid^2 \;\; . \tag{5.20}$$

Indeed,

$$\begin{aligned} \| u \|^2 \;= < u, u > \;&=\; < \sum_{I=1}^{\infty} < u, \psi_I > \psi_I, \sum_{J=1}^{\infty} < u, \psi_J > \psi_J > \\ &= \sum_{I=1}^{\infty} < u, \psi_I > \sum_{J=1}^{\infty} < u, \psi_J > < \psi_I, \psi_J > \\ &= \sum_{I=1}^{\infty} < u, \psi_I >^2 \;=\; \sum_{I=1}^{\infty} \mid \alpha_I \mid^2 \;\; . \end{aligned} \tag{5.21}$$

If $\{\phi_1, \phi_2, \ldots, \phi_N, \ldots\}$ are merely a countably infinite orthonormal set (i.e., not necessarily a basis), then

$$
\begin{aligned}
0 \;&\leq \|u \;-\; \sum_{I=1}^{N} < \phi_I, u > \phi_I\| \;\Leftrightarrow \\
0 \;&\leq \; < u \;-\; \sum_{I=1}^{N} < \phi_I, u > \phi_I, u \;-\; \sum_{J=1}^{N} < \phi_J, u > \phi_J > \Leftrightarrow \\
0 \;&\leq \; < u, u > \;-\; < u, \sum_{J=1}^{N} < \phi_J, u > \phi_J > \;-\; < \sum_{I=1}^{N} < \phi_I, u > \phi_I, u > \\
&\quad + \; \sum_{I=1}^{N} < \phi_I, u > \sum_{J=1}^{N} < \phi_J, u >< \phi_I, \phi_J > \Leftrightarrow \\
0 \;&\leq \|u\|^2 \;-\; 2 \sum_{I=1}^{N} < \phi_I, u >< \phi_I, u > \;+\; \sum_{I=1}^{N} < \phi_I, u >< \phi_I, u > \Leftrightarrow \\
0 \;&\leq \|u\|^2 \;-\; \sum_{I=1}^{N} \mid \alpha_I \mid^2, \qquad (5.22)
\end{aligned}
$$

and, since u does not depend on N,

$$
\sum_{I=1}^{\infty} \mid \alpha_I \mid^2 \leq \|u\|^2 \; . \qquad (5.23)
$$

The above result is known as *Bessel's inequality*.

The following theorem provides a clear connection between convergence in a Hilbert space and convergence of standard algebraic series.

Theorem

Let $\{\phi_1, \phi_2, \ldots, \phi_N, \ldots\}$ be a countably infinite orthonormal set in a Hilbert space $\mathcal{U}$. Then $\sum_{I=1}^{\infty} \alpha_I \phi_I$ converges in $\mathcal{U}$ if, and only if, $\sum_{I=1}^{\infty} \mid \alpha_I \mid^2$ converges.

Proof

To prove the preceding theorem, assume that the series $\sum_{I=1}^{\infty} \alpha_I \phi_I$ converges and write

$$
u \;=\; \sum_{I=1}^{\infty} \alpha_I \phi_I \; . \qquad (5.24)
$$

It follows from (5.23)

$$\sum_{I=1}^{\infty} \mid \alpha_I \mid^2 \leq \|u\|^2 \ , \tag{5.25}$$

which implies that $\sum_{I=1}^{\infty} \mid \alpha_I \mid^2$ is a bounded series of non-negative numbers, therefore converges.

Conversely, assume that $\sum_{I=1}^{\infty} \mid \alpha_I \mid^2$ converges and set

$$u_N \ = \ \sum_{I=1}^{N} \alpha_I \phi_I \ . \tag{5.26}$$

It follows that for any $N > M$

$$\|u_N \ - \ u_M\|^2 \ = < u_N \ - \ u_M, u_N \ - \ u_M > = \ \sum_{I=M+1}^{N} \ \mid \alpha_I \mid^2 \ , \tag{5.27}$$

therefore

$$\lim_{N,M \to \infty} \|u_N \ - \ u_M\| \ = \ 0 \ , \tag{5.28}$$

which implies that u_N is a Cauchy sequence. Since $\mathcal{U}$ is a Hilbert space (therefore is complete), it follows that u_N converges, namely the infinite series $\sum_{I=1}^{\infty} \alpha_I \phi_I$ is convergent.

The interpolation functions φ_I used in the finite element method should satisfy the *completeness* property in the space of admissible functions $\mathcal{U}$. This means that they have to be appropriately chosen from a family of functions $\{\varphi_I, \ I = 1, 2, \ldots\}$ which have the property that if $u \in \mathcal{U}$ and $< u, \varphi_I >= 0$ for all $I = 1, 2, \ldots$, then $u = 0$. It can be shown that in the context of Hilbert spaces, the completeness property is equivalent to satisfaction of Parseval's identity for any $u \in \mathcal{U}$. Also, completeness is equivalent to the requirement that any $u \in \mathcal{U}$ be expressed in a Fourier representation, as in (5.19).

In order to motivate the choice of φ_I's, recall the Weierstrass approximation theorem of elementary real analysis:

Weierstrass Approximation Theorem (1885)

Given a continuous function f in $[a, b] \subset \mathbb{R}$ and any scalar $\epsilon > 0$, there exists a polynomial P_N of degree N, such that

$$\mid f(x) \ - \ P_N(x) \mid < \ \epsilon \ , \tag{5.29}$$

for all $x \in [a, b]$.

The above theorem states that any continuous function f on a closed subset of $\mathbb{R}$ can be uniformly approximated by a polynomial function to within any desired level of accuracy. Using this theorem, one may conclude that the exact solution u to a given problem can be potentially approximated by a polynomial u_h of degree N, so that

$$\lim_{N\to\infty} \|u \; - \; u_h\| \; = \; 0 \; . \tag{5.30}$$

Polynomials in $\mathbb{R}$ (namely the sequence of functions 1, x, x^2, ...) satisfy the completeness property as stated earlier. The above theorem can be extended to polynomials defined in closed and bounded subsets of $\mathbb{R}^n$, as well as to trigonometric functions, as evidenced by the classical Fourier representation of a continuous real function u in the form

$$u(x) \; = \; \sum_{k=0}^{\infty} (\alpha_k \sin kx \; + \; \beta_I \cos kx) \; . \tag{5.31}$$

The interpolation functions are required to be complete, so that any smooth solution u be representable to within specified error by means of u_h. It should be noted that the preceding theorem does not guarantee that a numerical method, which involves complete interpolation functions, will necessarily provide a uniformly accurate approximate solution.

In certain occasions, properties (a), (b) and (e) of the interpolation functions are relaxed, in order to accommodate special requirements of the approximation.

5.2 Finite element spaces

The finite element method is a rational procedure for constructing local piece-wise polynomial interpolation functions, in accordance with the guidelines of the previous section. In order to initiate the discussion of the finite element method, introduce the notion of the finite element discretization: given the domain Ω of analysis, admit the existence of finite element sub-domains Ω^e, such that

$$\Omega \; = \; \overline{\bigcup_e \Omega^e} \; , \tag{5.32}$$

as shown schematically in Figure 5.1. Similarly, the boundary $\partial\Omega$ is decomposed into

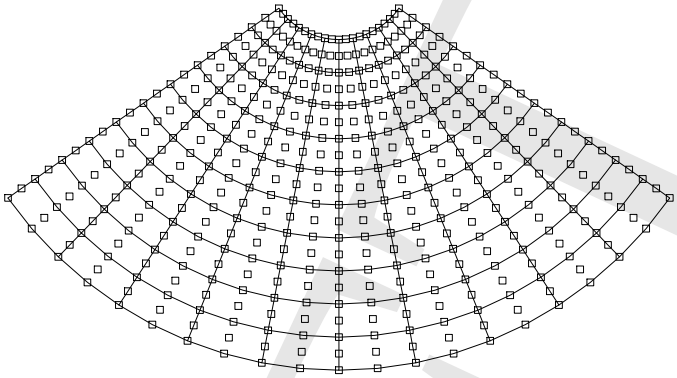

Figure 5.1: *A finite element mesh*

sub-domains $\partial\Omega^e$ consistently with (5.32), so that

$$\partial\Omega \subseteq \overline{\bigcup_e \partial\Omega^e} \,. \tag{5.33}$$

Also, admit the existence of points $I \in \Omega$, associated with sub-domains Ω^e. Points I have coordinates $\mathbf{x}_I$ with reference to a fixed coordinate system, and are referred to as the *nodal points* (or simply *nodes*). The collection of finite element sub-domains and nodal points within Ω (i.e., accounting for the specific geometry of the sub-domains and nodes) constitutes a *finite element mesh*. The geometry of each Ω^e is completely defined by the nodal points that lie on $\partial\Omega^e$ and in Ω^e.

Continuous piece-wise polynomial interpolation functions φ_I are defined for each interior finite element node I, so that, by convention,

$$\varphi_I(\mathbf{x}_J) = \begin{cases} 1 & \text{if } I = J \\ 0 & \text{otherwise} \end{cases} \,. \tag{5.34}$$

Similarly, one may define local interpolation functions for exterior boundary nodes that do not lie on the portion of the boundary where Dirichlet (or essential) conditions are enforced. The latter are satisfied locally by approximation functions which vanish at all other boundary and interior nodes. Moreover, the support of φ_I is restricted to the element domains in the immediate neighborhood of node I, as shown in Figure 5.2.

At this stage, it is possible to formally define a *finite element* as a mathematical object which consists of three basic ingredients:

(i) a finite element sub-domain Ω^e,

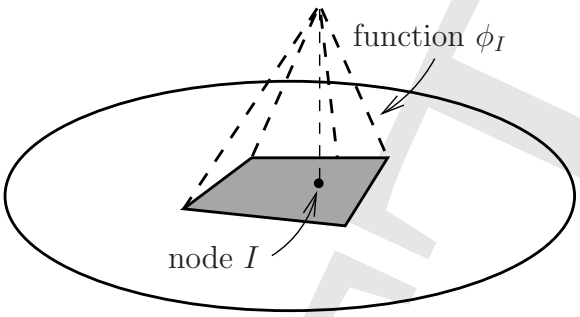

Figure 5.2: *A finite element-based interpolation function*

(ii) a linear space of interpolation functions, or more specifically, the restriction of the interpolation functions to Ω^e, and

(iii) a set of "degrees of freedom", namely those parameters α_I that are associated with non-vanishing interpolation functions in Ω^e.

Given the above general description of the finite element interpolation functions, one may proceed in establishing their admissibility in connection with the properties outlined in the preceding section.

Property (a) is generally satisfied by construction of the interpolation functions. Indeed, given any interior point P of Ω, there exist neighboring nodal points whose interpolation functions are non-zero at P. However, it is conceivable that (5.32) holds only approximately, i.e., subdomains Ω^e only partially cover the domain Ω, as seen in Figure 5.3. In this case, property (a) may be violated in certain small regions on the domain, thus inducing an error in the approximation.

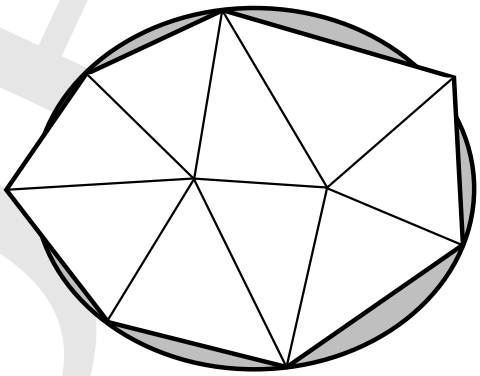

Figure 5.3: *Finite element vs. exact domain*

Property (b) is directly satisfied by fixing the degrees-of-freedom associated with the portion of the exterior boundary where Dirichlet (or essential) conditions are enforced. Again, an error in the approximation is introduced when the actual exterior boundary is not represented exactly by the finite element domain discretization, see Figure 5.4.

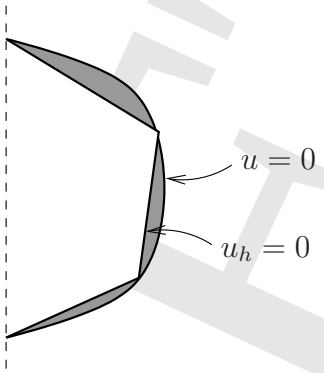

Figure 5.4: *Error in the enforcement of Dirichlet boundary conditions due to the difference between the exact and the finite element domain*

In order to show that property (c) is satisfied, assume, by contradiction, that for all $\mathbf{x} \in \Omega$, $u_h = 0$, while not all scalar parameters α_I are zero. Owing to (5.34), one may immediately conclude that at any node J

$$u_h(\mathbf{x}_J) \;=\; \sum_{I=1}^{N} \alpha_I \, \varphi_I(\mathbf{x}_J) \;=\; \alpha_J \;, \tag{5.35}$$

hence $\alpha_J = 0$. Since the nodal point J is chosen arbitrary, it follows that all α_J vanish, which constitutes a contradiction. Therefore, the proposed interpolation functions are linearly independent.

As already seen in Chapters 3 and 4, property (d) dictates that the admissible fields $\mathcal{U}_h$ and, if applicable, $\mathcal{W}_h$ must render the associated weak forms well-defined. In the finite element literature, this property is frequently referred to as the *compatibility condition*. The terminology stems from certain second-order differential equations of structural mechanics (e.g., the displacement-based equations of motion for linearly elastic solids), where integrability of the weak forms amounts to the requirement that the assumed displacement fields u_h belong to H^1. This, in turn, implies that the displacements should be "compatible", namely the displacements of individual finite elements domains should not exhibit overlaps or voids, as in Figure 5.5.

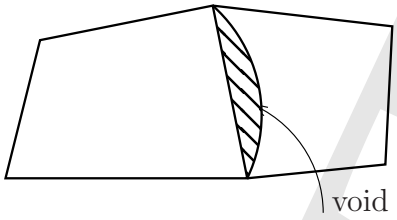

Figure 5.5: *A potential violation of the integrability (compatibility) requirement*

Property (e) and its implications within the context of the finite element method deserve special attention, and are discussed separately in the following section.

5.3 Completeness property

The completeness property requires that piecewise polynomial fields $\mathcal{U}_h$ contain "points" u_h that may uniformly approximate the exact solution u of a differential equation to within desirable accuracy. This approximation may be achieved by enriching $\mathcal{U}_h$ in various ways:

(a) Refinement of the domain discretization, while keeping the order of the polynomial interpolation fixed (*h-refinement*).

(b) Increase in the order of polynomial interpolation within a fixed domain discretization (*p-refinement*).

(c) Combined refinement of the domain discretization and increase of polynomial order of interpolation (*hp-refinement*).

(d) Repositioning of a domain discretization with fixed order of polynomial interpolation and element topology to enhance the accuracy of the approximation in a selective manner (*r-refinement*).

It can be shown that in order to assess completeness of a given finite element field, one must be able to conclude that the error in the approximation of the highest derivative of u in the weak form is at most of order $o(h)$, where h is a measure of the "fineness" of the approximation. To see this point, consider a smooth real function u, and fix a point x in its domain. With reference to Taylor's theorem, write

$$u(x+h) \;=\; u(x) \;+\; hu'(x) \;+\; \frac{1}{2!}h^2u''(x) \;+\; \ldots \;+\; \frac{1}{q!}h^q u^{(q)}(x) \;+\; o(h^{q+1}) \;, \qquad (5.36)$$

for any given $h > 0$. Assuming that $\mathcal{U}_h$ contains all polynomials in h that are complete to degree q, it follows that there exists a $u_h \in \mathcal{U}_h$ so that at $x + h$

$$u \;=\; u_h \;+\; o(h^{q+1}) \;. \tag{5.37}$$

Letting p be the order of the highest derivative of u in any weak form, it follows from (5.37) that

$$\frac{d^p u}{dx^p} \;=\; \frac{d^p u_h}{dx^p} \;+\; o(h^{q-p+1}) \;. \tag{5.38}$$

Thus, for $\mathcal{U}_h$ to be a (polynomially) complete field, it suffices to establish that

$$q - p + 1 \;\geq\; 1 \;, \tag{5.39}$$

or, equivalently,

$$q \;\geq\; p \;. \tag{5.40}$$

Indeed, in this case $\dfrac{d^p u_h}{dx^p}$ converges to $\dfrac{d^p u}{dx^p}$ as $h \to 0$ (i.e., under h-refinement). Hence, in order to guarantee completeness, any approximation to u must contain all polynomial terms of degree at least p. The same argument can be easily made for functions of several variables.

In the context of weighted residual methods, completeness guarantees that weak forms are computed to full resolution as the approximation becomes finer in the sense that $h \to 0$ (h-refinement) or $q \to \infty$ (p-refinement). Indeed, consider a weak form

$$B(w, u) \;+\; (w, f) \;+\; (w, \bar{q})_{\Gamma_q} \;=\; 0 \;, \tag{5.41}$$

associated with a linear partial differential equation and let both u_h and w_h be refined in the same fashion (i.e. using h- or p-refinement). It is easily seen that

$$B(w, u) \;=\; B(w_h, u_h) \;+\; B(w - w_h, u - u_h) \;+\; B(w - w_h, u_h) \;+\; B(w_h, u - u_h) \;. \tag{5.42}$$

Owing to (5.40), the last three terms on the right-hand side of the above identity are of order at least $o(h^{q-p+1})$ before integration. Taking the limit of the above identity as h approaches zero, it is desired that

$$B(w, u) \;=\; \lim_{h \to 0} B(w_h, u_h) \;. \tag{5.43}$$

under h-refinement. Likewise, taking the limit as $q \to \infty$, it is desired that

$$B(w, u) \;=\; \lim_{q \to \infty} B(w_h, u_h) \;. \tag{5.44}$$

under p-refinement. Both conditions hold true if condition (5.40) is satisfied.

Similar conclusions can be reached for the linear forms (w, f) and $(w, \bar{q})_{\Gamma_q}$.

Examples:

(a) Consider the differential equation

$$k\frac{d^2u}{dx^2} \;=\; f \quad \text{in } (0,1)\ ,$$

where $p = 1$ when using the Galerkin method (see Chapter 3). Then, (5.40) implies that all polynomial approximations of u should be complete up to linear terms in x, namely should contain independent monomials $\{1, x\}$.

(b) Consider the differential equation

$$\frac{\partial^4 u}{\partial x_1^4} \;+\; 2\frac{\partial^4 u}{\partial x_1^2 \partial x_2^2} \;+\; \frac{\partial^4 u}{\partial x_2^4} \;=\; f \quad \text{in } \Omega \subset \mathbb{R}^2\ ,$$

where it has been shown that a weak (variational) form is derivable such that $p = 2$. Then, the monomial terms that should be independently present in any complete approximation are $\{1, x_1, x_2, x_1^2, x_1x_2, x_2^2\}$.

Obviously, setting $q = p$ as in the preceding examples satisfies only the minimum requirement for completeness. Generally, the higher the order q relative to p, the richer the space of admissible functions $\mathcal{U}_h$. Thus, an increase in the order of completeness beyond the minimum requirements set by (5.40) yields more accurate approximations of the exact solution to a given problem.

A polynomial approximation in $\mathbb{R}^n$ is said to be *complete up to order* q, if it contains independently all monomials $x_1^{q_1}x_2^{q_2}\ldots x_n^{q_n}$, where $q_1 + q_2 + \ldots + q_n \leq q$. In $\mathbb{R}$, the above implies that terms $\{1, x, \ldots, x^q\}$ should be independently represented. In $\mathbb{R}^2$, completeness up to order q can be conveniently visualized by means of a *Pascal triangle*, as shown in Figure 5.6. In this case, the number of independent monomials is $\frac{(q+1)(q+2)}{2}$.

An alternative (and somewhat stronger) formalization of the completeness property can be obtained by noting that application of a weighted residual method to linear differential equation

$$A[u] \;=\; f \tag{5.45}$$

within *fixed* spaces $\mathcal{U}_h$ and, if necessary, $\mathcal{W}_h$, yields an approximate solution u_h typically obtained by solving a system of linear algebraic equations of the form (3.30). Therefore, for fixed h, one may define a *discrete* operator A_h associated with the operator A, so that

$$A_h[u] \;=\; A[u_h]\ , \tag{5.46}$$

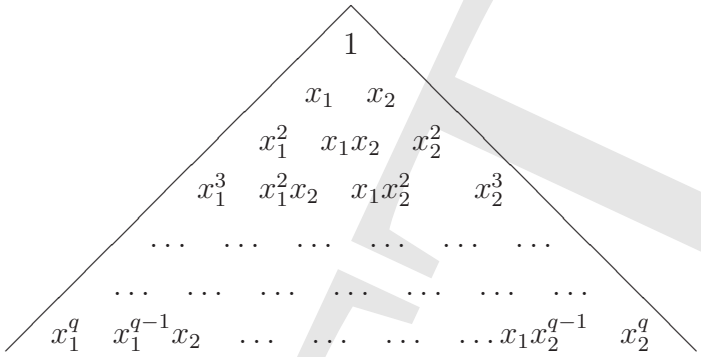

Figure 5.6: *Pascal triangle*

for any $u_h \in \mathcal{U}_h$. Subsequently, the domain of the discrete operator can be appropriately extended, so that it encompasses the whole space $\mathcal{U}$. Then, completeness implies that

$$A_h[u] \;=\; f \;+\; o(h^\alpha) \quad ; \quad \alpha > 0 \,. \tag{5.47}$$

Assuming sufficient smoothness of u, equation (5.47) implies that the discrete operator A_h converges to the continuous operator A as h approaches zero.

5.4 Basic finite element shapes in one, two and three dimensions

The geometric shape of a finite element domain Ω^e can be fully determined by two sets of data:

(i) The position of nodal points.

(ii) A domain interpolation procedure, which may coincide with the interpolation employed for the dependent variables of the problem.

Thus, the position vector $\mathbf{x}$ of a point in Ω^e can be written as a function of the position vectors $\mathbf{x}_I$ of nodes I and the given domain interpolation functions.

5.4.1 One dimension

One-dimensional finite element domains are line segments, straight or curved, as in Figure 5.7.

Figure 5.7: *Finite element domains in one dimension*

5.4.2 Two dimensions

Two-dimensional finite element domains are typically triangular or quadrilateral, with straight or curved edges, as in Figure 5.8. Elements with more complicated geometric shapes are rarely used in practice.

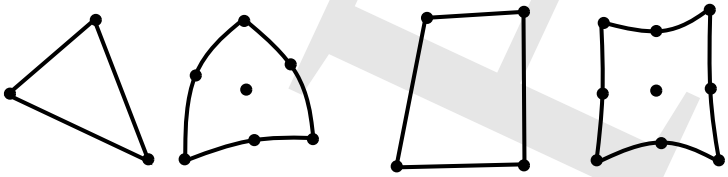

Figure 5.8: *Finite element domains in two dimensions*

5.4.3 Three dimensions

The most useful three-dimensional finite element domains are tetrahedral (tets), pentahedral (pies) and hexahedral (bricks), with straight or curved edges and flat or non-flat faces, see Figure 5.9. Again, elements with more complicated geometric shapes are generally avoided.

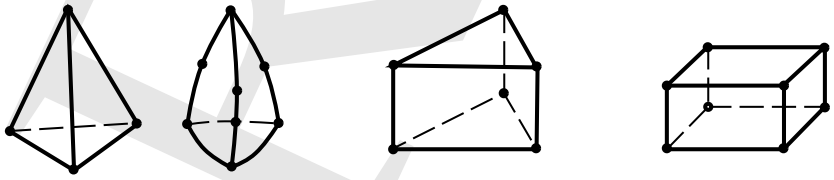

Figure 5.9: *Finite element domains in three dimensions*

5.4.4 Higher dimensions

Elements in four or higher dimensions will not be discussed here.

5.5 Polynomial shape functions

Element interpolation functions are generally used for two purposes, namely to generate an approximation for the dependent variable and to parametrize the element domain. The second use of these functions justifies their frequent identification as *shape* functions. In what follows, polynomial element interpolation functions are visited in connection with the construction of finite element approximations in one, two and three dimensions.

5.5.1 Interpolations in one dimension

First, consider the case of continuous piecewise polynomial interpolation functions. These functions are admissible for the Galerkin-based finite element approximations associated with the solution of the one-dimensional counterpart of the Laplace-Poisson equation discussed in earlier sections. Furthermore, assume that the order of the highest derivative in the weak form is $p = 1$, so that the completeness requirement necessitates the construction of a polynomial approximation which is complete to degree $q \geq 1$.

The simplest finite element which satisfies the above integrability and completeness requirements is the 2-node element of length Δx, as in Figure 5.10. Associated with every such element, there is a local node numbering system and a coordinate system x (here having its origin at node 1). The interpolation u_h of the dependent variable u in the element domain Ω^e takes the form

$$u_h(x) \;=\; N_1^e(x)\, u_1^e + N_2^e(x)\, u_2^e \;, \tag{5.48}$$

where the element interpolation functions N_1^e and N_2^e are defined as

$$N_1^e(x) \;=\; 1 - \frac{x}{\Delta x} \quad , \qquad N_2^e(x) \;=\; \frac{x}{\Delta x} \;. \tag{5.49}$$

It is immediately noted that $N_1^e(0) = 1$ and $N_1^e(\Delta x) = 0$, while $N_2^e(0) = 0$ and $N_2^e(\Delta x) = 1$.

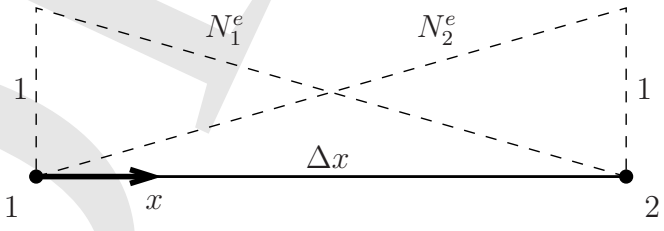

Figure 5.10: *Linear element interpolations in one dimension*

Also, u_1^e and u_2^e in (5.48) denote the element "degrees of freedom", which, given the form

of the element interpolation functions, can be directly identified with the ordinates of the dependent variable at nodes 1 and 2 (numbered locally as shown in Figure 5.10), respectively.

Clearly, the above finite element approximation is complete in 1 and x (i.e., $q = 1$). In addition, it satisfies the compatibility requirement by construction, since the dependent variable is continuous in Ω^e, as well as at all interelement boundaries. The last conclusion can be reached by noting that the nodal degrees of freedom are shared when the nodes themselves are shared between contiguous elements.

A complete quadratic interpolation can be obtained by constructing 3-node elements, as in Figure 5.11. Here, the dependent variable is given by

$$u_h(x) \;=\; N_1^e(x)\, u_1^e + N_2^e(x)\, u_2^e + N_3^e(x)\, u_3^e \;, \tag{5.50}$$

where

$$N_1^e(x) \;=\; \frac{(x-\Delta x)(x-2\Delta x)}{2\Delta x^2} \quad , \quad N_2^e(x) \;=\; \frac{x(x-\Delta x)}{2\Delta x^2} \quad , \quad N_3^e(x) \;=\; -\frac{x(x-2\Delta x)}{\Delta x^2} \;. \tag{5.51}$$

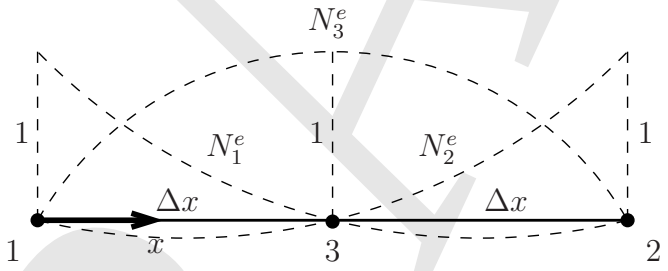

Figure 5.11: *Standard quadratic element interpolations in one dimension*

Again, compatibility and completeness (to degree $q = 2$) are satisfied by the interpolation in (5.50).

Generally, for an element with $q+1$ nodes having coordinates x_i, $i = 1, \ldots, q+1$, one may obtain a *Lagrangian interpolation* of the form

$$u_h(x) \;=\; \sum_{i=1}^{q+1} N_i^e(x) u_i^e \;. \tag{5.52}$$

The generic element interpolation function N_i^e is a polynomial of degree q written as

$$N_i^e(x) \;=\; a_0 \;+\; a_1 x \;+\; \ldots \;+\; a_q x^q \;, \tag{5.53}$$

where

$$N_i^e(x_j) \;=\; \begin{cases} 1 & \text{if } i = j \\ 0 & \text{if } i \neq j \end{cases} \;. \tag{5.54}$$

Conditions (5.54) give rise to a system of $q+1$ equations for the $q+1$ parameters c_0 to c_q. Interestingly, a direct solution of this system is not necessary to determine the explicit functional form of N_i^e. Indeed, it can be immediately verified that

$$N_i^e(x) \;=\; l_i(x) \;=\; \frac{(x \;-\; x_1)\ldots(x \;-\; x_{i-1})(x \;-\; x_{i+1})\ldots(x \;-\; x_{q+1})}{(x_i \;-\; x_1)\ldots(x_i \;-\; x_{i-1})(x_i \;-\; x_{i+1})\ldots(x_i \;-\; x_{q+1})} \;. \tag{5.55}$$

The above general procedure by way of which the degree of polynomial completeness is progressively increased by adding nodes and associated degrees of freedom is referred to as *standard* interpolation. An alternative to this procedure is provided by the so-called *hierarchical* interpolation. To illustrate an application of hierarchical interpolation, consider the 2-node element discussed earlier in this section, and modify (5.48) so that

$$u_h(x) \;=\; N_1^e(x)\, u_1^e + N_2^e(x)\, u_2^e + \tilde{N}_3^e(x)\, \alpha^e \;, \tag{5.56}$$

where both the function $\tilde{N}_3^e$ and the degree of freedom α^e are to be determined. Clearly, $\tilde{N}_3^e$ should be a quadratic function of x, since a complete linear interpolation is already guaranteed by the original form of u_h in (5.48). Therefore,

$$\tilde{N}_3^e(x) \;=\; a_0 \;+\; a_1 x \;+\; a_2 x^2 \;, \tag{5.57}$$

where a_0, a_1 and a_2 are parameters to be determined. In order to satisfy compatibility (i.e., continuity of u_h at interelement boundaries), it is sufficient to assume that $\tilde{N}_3^e(0) = 0$ and $\tilde{N}_3^e(\Delta x) = 0$. These conditions imply that

$$\tilde{N}_3^e(x) \;=\; \frac{ax}{\Delta x}\,(1 \;-\; \frac{x}{\Delta x}) \;, \tag{5.58}$$

where a can be any non-zero constant. The three interpolation functions obtained by the above hierarchical procedure are depicted in Figure 5.12. In contrast with the standard interpolation, here the degree of freedom α^e is not associated with a finite element node. A simple algebraic interpretation of α^e can be obtained as follows: let the element interpolation function $\tilde{N}_3^e(x)$ take the specific form

$$\tilde{N}_3^e(x) \;=\; \frac{4x}{\Delta x}\,(1 \;-\; \frac{x}{\Delta x}) \;. \tag{5.59}$$

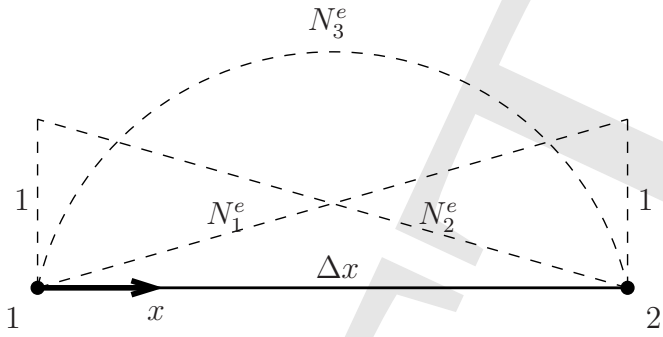

Figure 5.12: *Hierarchical quadratic element interpolations in one dimension*

Then, it can be trivially concluded that α^e quantifies the deviation from linearity of u_h at the mid-point of Ω^e, namely at $x = \Delta x/2$.

Remark:

- By construction, the degree of freedom α^e is not shared between contiguous elements. Consequently, it is possible to determine its value locally (i.e., at the element level), as a function of the other element degrees of freedom. As a result, α^e does not need to enter the global system of equations. In the structural mechanics literature, the process of locally eliminating hierarchical degrees of freedom at the element level is referred to as *static condensation*.

Finite element approximations that maintain continuity of the first derivative of the dependent variable are necessary for the solution of certain higher-order partial differential equations. As a representative example, consider the fourth-order differential equation $\dfrac{d^4u}{dx^4} = f$, which, after application of the Bubnov-Galerkin method gives rise to a weak form that involves second-order derivatives of both the dependent variable and the weighting function. Here, continuity of the first derivative of u is sufficient to guarantee well-posedness of the weak form. In addition, the completeness requirement is met by ensuring that the approximation in each element is polynomially complete to degree $q \geq 2$.

A simple element which satisfies the above requirements is the 2-node element of Figure 5.13, in which each node is associated with two degrees of freedom, identified as the ordinates of the dependent variable u and its first derivative $\theta = \dfrac{du}{dx}$, respectively.

Given that there are four degrees of freedom in each element, a cubic polynomial interpolation of the form

$$u_h(x) \;=\; c_0 \;+\; c_1 x \;+\; c_2 x^2 \;+\; c_3 x^3 \tag{5.60}$$

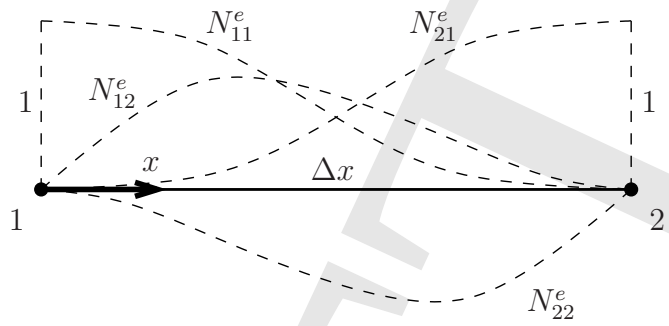

Figure 5.13: *Hermitian interpolation functions in one dimension*

can be determined uniquely under the conditions

$$u_h(0) \;=\; u_1^e \quad , \quad \frac{du_h}{dx}(0) \;=\; \theta_1^e \quad , \quad u_h(\Delta x) \;=\; u_2^e \quad , \quad \frac{du_h}{dx}(\Delta x) \;=\; \theta_2^e \; . \tag{5.61}$$

Solving the above equations for the four parameters c_0 to c_3 yields a standard *Hermitian interpolation*, in which

$$u_h(x) \;=\; \sum_{i=1}^{2} N^e_{i1}(x)\, u_i^e \;+\; \sum_{i=1}^{2} N^e_{i2}(x)\, \theta_i^e \; , \tag{5.62}$$

where

$$\begin{aligned} N^e_{11} \;&=\; 1 \;-\; 3\,\big(\frac{x}{\Delta x}\big)^2 \;+\; 2\,\big(\frac{x}{\Delta x}\big)^3 \qquad , \qquad N^e_{21} \;=\; 3\,\big(\frac{x}{\Delta x}\big)^2 \;-\; 2\,\big(\frac{x}{\Delta x}\big)^3 \\ N^e_{12} \;&=\; \Delta x\Big[\frac{x}{\Delta x} \;-\; 2\,\big(\frac{x}{\Delta x}\big)^2 \;+\; \big(\frac{x}{\Delta x}\big)^3\Big] \qquad , \qquad N^e_{22} \;=\; \Delta x\Big[-\,\big(\frac{x}{\Delta x}\big)^2 \;+\; \big(\frac{x}{\Delta x}\big)^3\Big] \; . \end{aligned} \tag{5.63}$$

Generally, a Hermitian interpolation can be introduced for a $q+1$-node element, where each node i is associated with coordinate x_i and with degrees of freedom u_i^e and θ_i^e. It follows that u_h is a polynomial of degree $2q+1$ in the form

$$u_h(x) \;=\; \sum_{i=1}^{q+1} N^e_{i1}(x)\, u_i^e \;+\; \sum_{i=1}^{q+1} N^e_{i2}(x)\, \theta_i^e \; . \tag{5.64}$$

The element interpolation functions N^e_{i1} in the above equation satisfy

$$N^e_{i1}(x_j) \;=\; \begin{cases} 1 & \text{if } i = j \\ 0 & \text{if } i \neq j \end{cases} \qquad , \qquad \frac{dN^e_{i1}}{dx}(x_j) \;=\; 0 \; . \tag{5.65}$$

Similarly, the functions N^e_{i2} satisfy the conditions

$$N^e_{i2}(x_j) \;=\; 0 \quad , \quad \frac{dN^e_{i2}}{dx}(x_j) \;=\; \begin{cases} 1 & \text{if } i = j \\ 0 & \text{if } i \neq j \end{cases} \; . \tag{5.66}$$

It can be easily verified that the above *Hermitian polynomials* are defined as

$$N^e_{i1}(x) \;=\; \big[1 \;-\; 2l'_i(x_i)\,(x \;-\; x_i)\big]\,l^2_i(x) \qquad , \qquad N^e_{i2}(x) \;=\; (x \;-\; x_i)\,l^2_i(x)\;, \tag{5.67}$$

where $l_i(x)$ denotes the Lagrangian polynomial of degree q defined in (5.55). The above interpolation satisfies continuity of the dependent variable and its first derivative across interelement boundaries. In addition, it guarantees polynomial completeness up to degree $q = 3$.

Higher-order accurate elements can be also constructed starting from the 2-node element and adding hierarchical degrees of freedom. For example, one may assume a quartic interpolation of the form

$$u_h(x) \;=\; \sum_{i=1}^{2} N^e_{i1}(x)\,u^e_i \;+\; \sum_{i=1}^{2} N^e_{i2}(x)\,\theta^e_i \;+\; \tilde{N}^e_5(x)\,\alpha^e, \tag{5.68}$$

where the interpolation function $\tilde{N}^e_5$ is written as

$$\tilde{N}^e_5(x) \;=\; a_0 \;+\; a_1 x \;+\; a_2 x^2 \;+\; a_3 x^3 \;+\; a_4 x^4\;. \tag{5.69}$$

Given the conditions $\tilde{N}^e_5(0) = \tilde{N}^e_5(\Delta x) = 0$ and $\dfrac{d\tilde{N}^e_5}{dx}(0) = \dfrac{d\tilde{N}^e_5}{dx}(\Delta x) = 0$, it follows that

$$\tilde{N}^e_5(x) \;=\; a\Big[\big(\frac{x}{\Delta x}\big)^2 \;-\; 2\,\big(\frac{x}{\Delta x}\big)^3 \;+\; \big(\frac{x}{\Delta x}\big)^4\Big]\;. \tag{5.70}$$

Finite element approximations which enforce continuity of higher-order derivatives are conceptually simple. The idea is to introduce degrees of freedom identified with the dependent variable and its derivatives up to the highest order in which continuity is desired. However, such elements are rarely used in practice and will not be discussed here in detail.

5.5.2 Interpolations in two dimensions

First, consider finite element interpolations in two dimensions, where continuity of the dependent variable across interelement boundaries is sufficient to satisfy the compatibility requirement, while polynomial completeness is necessary only to degree $p = 1$. It can be easily verified that the above requirements lead to a proper finite element approximation of the Laplace-Poisson equation discussed in connection with the Galerkin method in Section 3.2.

The simplest two-dimensional element is the 3-node straight-edge triangle Ω^e with one degree-of-freedom per node, as seen in Figure 5.14. For this element, assume a linear poly-

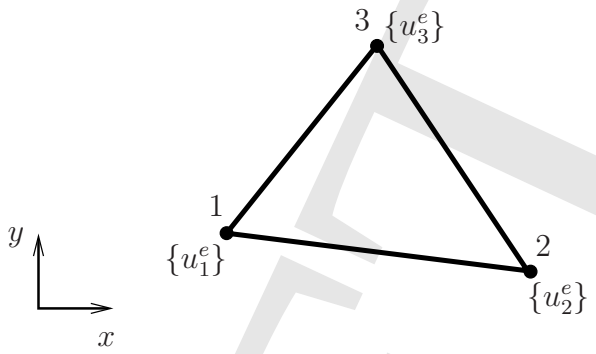

Figure 5.14: *A 3-node triangular element*

nomial interpolation u_h of the dependent variable u in the form

$$u_h(x,y) \;=\; \sum_{i=1}^{3} N_i^e(x,y) u_i^e \;=\; c_0 \;+\; c_1 x \;+\; c_2 y \;, \tag{5.71}$$

with reference to a fixed Cartesian coordinate system (x, y). Upon identifying the degrees of freedom at each node $i = 1, 2, 3$ having coordinates (x_i, y_i) with the ordinate u_i^e of the dependent variable at that node, one obtains a system of three linear algebraic equations with unknowns c_0, c_1 and c_2, in the form

$$\begin{aligned} u_1^e \;&=\; c_0 \;+\; c_1 x_1 \;+\; c_2 y_1 \;, \\ u_2^e \;&=\; c_0 \;+\; c_1 x_2 \;+\; c_2 y_2 \;, \\ u_3^e \;&=\; c_0 \;+\; c_1 x_3 \;+\; c_2 y_3 \;. \end{aligned} \tag{5.72}$$

Assuming that the solution of the above system is unique, one may write

$$\begin{aligned} c_0 \;&=\; \frac{1}{2A}\Big[u_1^e(x_2 y_3 \;-\; x_3 y_2) \;+\; u_2^e(x_3 y_1 - x_1 y_3) \;+\; u_3^e(x_1 y_2 - x_2 y_1)\Big] \;, \\ c_1 \;&=\; \frac{1}{2A}\Big[u_1^e(y_2 \;-\; y_3) \;+\; u_2^e(y_3 \;-\; y_1) \;+\; u_3^e(y_1 \;-\; y_2)\Big] \;, \\ c_2 \;&=\; \frac{1}{2A}\Big[u_1^e(x_3 \;-\; x_2) \;+\; u_2^e(x_1 \;-\; x_3) \;+\; u_3^e(x_2 \;-\; x_1)\Big] \;, \end{aligned} \tag{5.73}$$

where

$$A \;=\; \frac{1}{2}\det\begin{bmatrix} 1 & x_1 & y_1 \\ 1 & x_2 & y_2 \\ 1 & x_3 & y_3 \end{bmatrix} . \tag{5.74}$$

It is interesting to note that A represents the (signed) area of the triangle Ω^e. Therefore, the system (5.72) is solvable if, and only if, the nodes 1,2,3 do not lie on the same line. In

addition, it can be easily concluded that the area A of a non-degenerate triangle is positive if, and only if, the nodes are numbered in a counter-clockwise manner, as in Figure 5.14.

Explicit polynomial expressions for the element interpolation functions are obtained from (5.71) and (5.73) in the form

$$\begin{aligned} N_1^e &= \frac{1}{2A}\Big[(x_2y_3 - x_3y_2) + (y_2 - y_3)x + (x_3 - x_2)y\Big] \\ N_2^e &= \frac{1}{2A}\Big[(x_3y_1 - x_1y_3) + (y_3 - y_1)x + (x_1 - x_3)y\Big] \\ N_3^e &= \frac{1}{2A}\Big[(x_1y_2 - x_2y_1) + (y_1 - y_2)x + (x_2 - x_1)y\Big] \end{aligned} \quad . \tag{5.75}$$

It can be noted from $(5.75)_1$ that $N_1^e(x,y) = 0$ coincides with the equation of the straight line passing through nodes 2 and 3. This observation is sufficient to guarantee continuity of u_h across interelement boundaries. Indeed, since N_1^e vanishes identically along 2-3, the interpolation u_h, which varies linearly along this line, is fully determined as a function of the degrees-of-freedom u_2^e and u_3^e. These degrees-of-freedom, in turn, are shared between the elements with common edge 2-3, which establishes the continuity of u_h as the edge 2-3 is crossed between these two elements. Obviously, entirely analogous arguments apply to edges 3-1 and 1-2. Furthermore, completeness to degree $q = 1$ is satisfied, since any linear polynomial function of x and y can be uniquely represented by three parameters, such as u_i^e, $i = 1, 2, 3$, and can be spanned over Ω^e by the interpolation functions in (5.75).

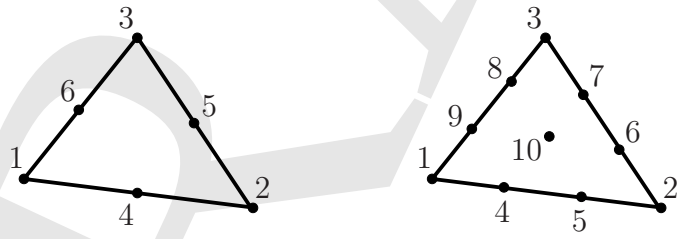

Figure 5.15: *Higher-order triangular elements*

Triangular elements with polynomial order of completeness $q \geq 1$ can be constructed by adding nodes accompanied by degrees-of-freedom to the straight-edge triangle. Examples of 6- and 10-node triangular elements which are polynomially complete to degree $q = 2$ and 3 are illustrated in Figure 5.15. It should be noted that the nodes are generally positioned with geometric regularity. Thus, for the 6-node triangle, the nodes are located at the corners and the mid-edges of the triangular domain. Again, the element interpolation functions can be determined by the procedure followed earlier for the 3-node triangle. Similarly, continuity

of the dependent variable in these elements can be proved by arguments identical to those used for the 3-node triangle. Elements featuring irregular positioning of the nodes, such as the 4-node element in Figure 5.16 are typically not desirable, as they produce a biased interpolation of the dependent variable without appreciably contributing towards increasing the polynomial degree of completeness. Such elements are sometimes used as "transitional" interfaces intended to properly connect meshes of different types of elements (e.g., a mesh consisting of 3-node triangles with another consisting of 6-node triangles).

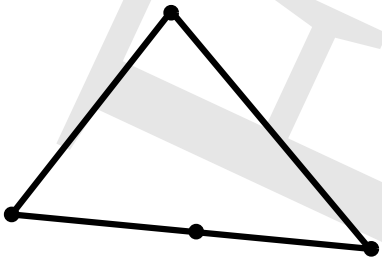

Figure 5.16: *A transitional triangular element*

In the study of triangular elements, it is analytically advantageous to introduce an alternative coordinate representation and use it instead of the standard Cartesian representation introduced earlier in this section. To this end, note that an arbitrary interior point of Ω^e with Cartesian coordinates (x, y) divides the element domain into three triangular sub-regions with areas A_1, A_2 and A_3, as shown in Figure 5.17. Noting that

$$A_1 \;=\; \frac{1}{2}\det\begin{bmatrix} 1 & x & y \\ 1 & x_2 & y_2 \\ 1 & x_3 & y_3 \end{bmatrix} \;, \tag{5.76}$$

with similar expressions for A_2 and A_3, define the so-called area coordinates of the point (x, y) as

$$L_i \;=\; \frac{A_i}{A} \quad , \quad i = 1, 2, 3 \;. \tag{5.77}$$

Clearly, only two of the three *area coordinates* are independent since it is seen from (5.77) that $L_1 + L_2 + L_3 = 1$. Interestingly, comparing (5.75) to (5.77) it is immediately apparent that $N_i^e = L_i$, $i = 1, 2, 3$. Generally, the area coordinates can vastly simplify the calculation of element interpolation functions in straight-edge triangular elements. With reference to the 6-node element depicted in Figure 5.15, note that the area coordinate representation of node 1 is $(1, 0, 0)$, while that of node 4 is $(\frac{1}{2}, \frac{1}{2}, 0)$. The representation of the edge 2-3

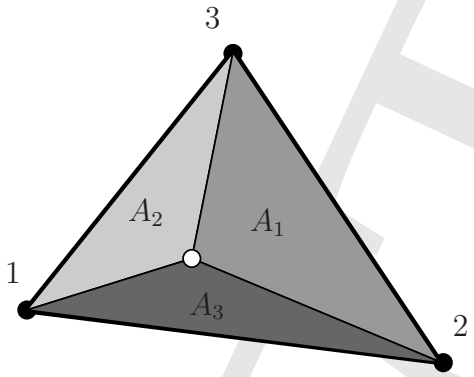

Figure 5.17: *Area coordinates in a triangular domain*

is $L_1 = 0$ (or, equivalently, $L_2 + L_3 = 1$), while that of the line connecting nodes 5 and 6 is $L_3 = \frac{1}{2}$. Given the above, the six element interpolation functions of this element can be expressed in terms of the area coordinates as

$$N_1^e \;=\; 2L_1(L_1 \;-\; \frac{1}{2}) \quad , \quad N_2^e \;=\; 2L_2(L_2 \;-\; \frac{1}{2}) \quad , \quad N_3^e \;=\; 2L_3(L_3 \;-\; \frac{1}{2})$$
$$N_4^e \;=\; 4L_1L_2 \quad , \quad N_5^e \;=\; 4L_2L_3 \quad , \quad N_6^e \;=\; 4L_3L_1 \; . \tag{5.78}$$

An important formula for the integration of polynomial functions of the area coordinates over the region of a straight-edge triangle can be established in the form

$$\int_{\Omega^e} L_1^\alpha L_2^\beta L_3^\gamma \, dA \;=\; \frac{\alpha!\,\beta!\,\gamma!}{(\alpha \,+\, \beta \,+\, \gamma \,+\, 2)!}\, 2A \; , \tag{5.79}$$

where α, β and γ are integers.

Quadrilateral elements are also used widely in finite element practice. First, attention is focused on the special case of rectangular elements for $p = 1$. The simplest possible such element is the 4-node rectangle of Figure 5.18. Here, it is assumed that the dependent variable is interpolated as

$$u_h \;=\; \sum_{i=1}^{4} N_i^e u_i^e \;=\; c_0 + c_1 x + c_2 y + c_3 xy \; , \tag{5.80}$$

where u_i^e, $i = 1 - 4$, are the nodal degrees of freedom (corresponding to the ordinates of the dependent variable at the nodes) and $c_0 - c_3$ are constants. Following the process outlined

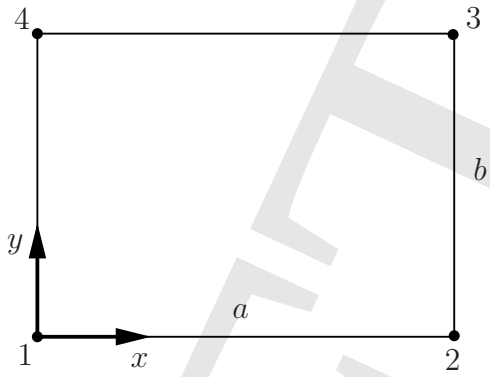

Figure 5.18: *Four-node rectangular element*

earlier, one may determine these constants by requiring that

$$\begin{aligned} u_1^e &= c_0 + c_1 x_1^e + c_2 y_1^e + c_3 x_1^e y_1^e \ , \\ u_2^e &= c_0 + c_1 x_2^e + c_2 y_2^e + c_3 x_2^e y_2^e \ , \\ u_3^e &= c_0 + c_1 x_3^e + c_2 y_3^e + c_3 x_3^e y_3^e \ , \\ u_4^e &= c_0 + c_1 x_4^e + c_2 y_4^e + c_3 x_4^e y_4^e \ . \end{aligned} \tag{5.81}$$

As before, the solution of the preceding linear system yields expressions for $c_0 - c_3$, which, in turn, can be used in connection with (5.80) to establish expressions for N_i^e, $i = 1 - 4$. However, it is rather simple to deduce these expressions directly by exploiting the fundamental property of the shape functions, namely that they vanish at all nodes except for one where they attain unit value. Indeed, in the case of the 4-node rectangle of Figure 5.18, these functions are given by

$$\begin{aligned} N_1^e &= \frac{1}{ab}(x-a)(y-b) \ , \\ N_2^e &= -\frac{1}{ab}x(y-b) \ , \\ N_3^e &= \frac{1}{ab}xy \ , \\ N_4^e &= -\frac{1}{ab}(x-a)y \ . \end{aligned} \tag{5.82}$$

The completeness property of this element is readily apparent, as one may represent any polynomial with terms $\{1, x, y, xy\}$[2]. Integrability is also guaranteed; indeed, taking any element edge, say, for example, edge 1-2, it is clear that $N_3^e = N_4^e = 0$. Hence, along this

[2]Note that the degree of completeness is still only $q = 1$ despite the presence of the bilinear term xy.

edge u_h is a linear function fully determined by the values of u_1^e and u_2^e, which, it turn, are shared with the neighboring element on the other side of edge 1-2.

Higher-order rectangular elements can be divided into two families based on the methodology used to generate them: these are the *serendipity* and the *Lagrangian* elements. The 4-node rectangle is common to both families. The next three elements of the serendipity family are the 8-, 12- and 17-node elements, see Figure 5.19. These elements are polynomially complete to degree $q = 2, 3$ and 4, respectively. The 8-node rectangle may represent any

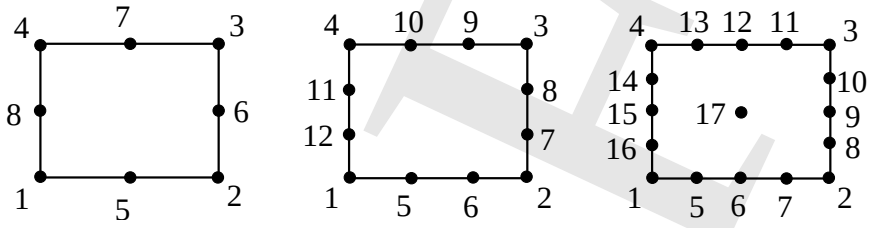

Figure 5.19: *Three members of the serendipity family of rectangular elements*

polynomial with terms $\{1, x, y, x^2, xy, y^2, x^2y, xy^2\}$. This can be either assumed at the outset (following the approach used earlier for the 4-node rectangle) and confirmed by enforcing the restrictions $u_h(x_i, y_i) = u_i^e$, $i = 1 - 8$, or by directly "guessing" the mathematical form of the shape functions using their fundamental property. Regrettably, this guessing becomes more difficult for the 12- and the 17-node elements, which explains the characterization of this family as "serendipity". It can be shown that for a rectangular element of the serendipity family with $m + 1$ nodes per edge, the represented monomials in Pascal's triangle are as shown in Figure 5.20.

$$
\begin{array}{ccccc}
 & & 1 & & \\
 & & x \quad y & & \\
 & . & xy & . & \\
 & . \quad & . \quad & . \quad & . \\
 & . \quad & . \quad & . \quad & . \\
x^m & . & & . & y^m \\
x^m y & & & & xy^m
\end{array}
$$

Figure 5.20: *Pascal's triangle for serendipity elements (before accounting for any interior nodes)*

The Lagrangian family of rectangular elements is comprised of the 4-node element discussed earlier, followed by the 9-, 16- and 25-node element, see Figure 5.21. The 9-node rect-

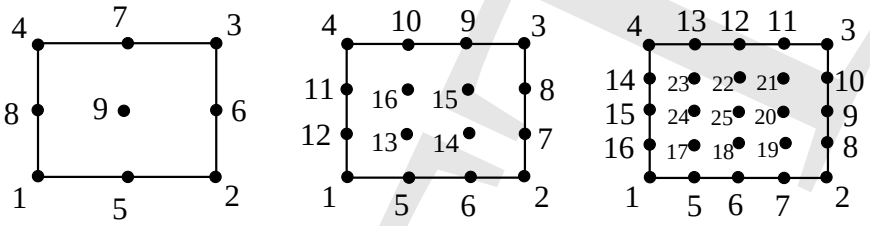

Figure 5.21: *Three members of the Lagrangian family of rectangular elements*

angle is capable of representing any polynomial with terms $\{1, x, y, x^2, xy, y^2, x^2y, xy^2, x^2y^2\}$. In contrast to the serendipity elements, the shape functions of the Lagrangian elements can be determined trivially as products of one-dimensional Lagrange interpolation functions. As an example, consider the shape function N^e_{18} associated with node 18 of the 25-node element of Figure 5.21. This can be written as

$$N^e_{18} \;=\; l_3(x) l_2(y) \;, \tag{5.83}$$

where

$$\begin{aligned} l_3(x) \;&=\; \frac{(x - x_{16})(x - x_{17})(x - x_{19})(x - x_8)}{(x_{18} - x_{16})(x_{18} - x_{17})(x_{18} - x_{19})(x_{18} - x_8)} \;, \\ l_2(y) \;&=\; \frac{(y - y_6)(y - y_{25})(y - x_{22})(y - y_{12})}{(y_{18} - y_6)(y_{18} - y_{25})(y_{18} - y_{22})(y_{18} - y_{12})} \;. \end{aligned} \tag{5.84}$$

Again, it is straightforward to see that for a rectangular element of the Lagrangian family with $m + 1$ nodes per edge, the represented monomials in Pascal's triangle are as shown in Figure 5.22.

All serendipity and Lagrangian rectangular elements are invariant under 90^o rotations, meaning that they represent the same monomial terms in x and y. This is clear from the symmetry in x and y of the represented monomials in the associated Pascal triangles of Figure 5.20 and Figure 5.22.

General quadrilaterals, such as the 4-node element in Figure 5.23, present a difficulty. In particular, it is easy to see that if one assumes at the outset a bilinear interpolation as in equation (5.80), then the value of u_h along a given edge generally depends not only on the nodal values at the two end-points of the edge, but also on the other two nodal values, which immediately implies violation of the interelement continuity of u_h. If, on the other hand, one

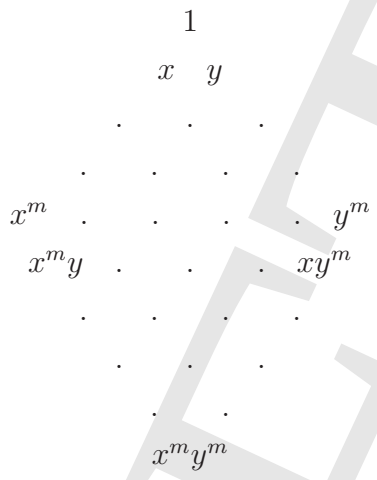

Figure 5.22: *Pascal's triangle for Lagrangian elements*

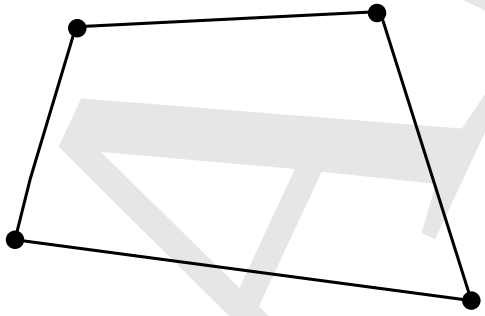

Figure 5.23: *A general quadrilateral finite element domain*

constructs a set of shape functions that satisfy the fundamental property, then it is easily seen that these functions are not complete to the minimum degree $q = 1$. One simple way to circumvent this difficulty is to construct a composite 4-node rectangle consisting of two connected triangles or a composite 5-node triangle consisting of four connected triangles, as in Figure 5.24. In both cases, the interpolation in each triangle is linearly complete and continuity of the dependent variable is guaranteed at all interelement boundaries. In a subsequent section, the question of general quadrilateral elements will be revisited within the context of the so-called isoparametric mapping.

The construction of two-dimensional finite elements with $p = 2$ is substantially more complicated than the respective one-dimensional case. To illustrate this point, consider a simple cubically complete interpolation of the dependent variable u_h as

$$u_h \;=\; c_0 + c_1 x + c_2 y + c_3 x^2 + c_4 xy + c_5 y^2 + c_6 x^3 + c_7 x^2 y + c_8 x y^2 + c_9 y^3 \;. \qquad (5.85)$$

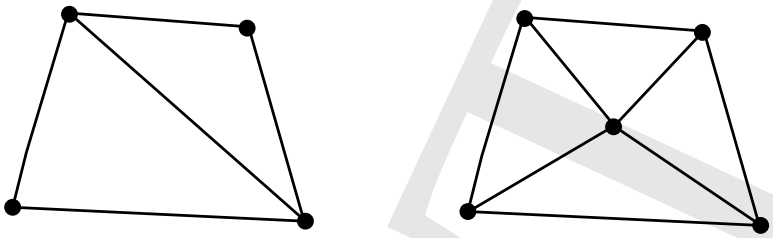

Figure 5.24: *Rectangular finite elements made of two or four joined triangular elements*

One may choose to associate this interpolation with the 3-node triangular element in Figure 5.25. Here, there are three degrees of freedom per node, namely the dependent variable u_h and its two partial derivatives $\dfrac{\partial u_h}{\partial x}$ and $\dfrac{\partial u_h}{\partial y}$. Given that there are 10 unknown coefficients c_i, $i = 0-9$, and only 9 degrees of freedom, one has to either add an extra degree of freedom or restrict the interpolation. The former may be accomplished by adding a fourth node at the centroid of the triangle and assigning the degree of freedom to be equal to the ordinate of the dependent variable at that point. The latter may be effected by requiring the monomials x^2y and xy^2 to have the same coefficient, i.e., $c_7 = c_8$.

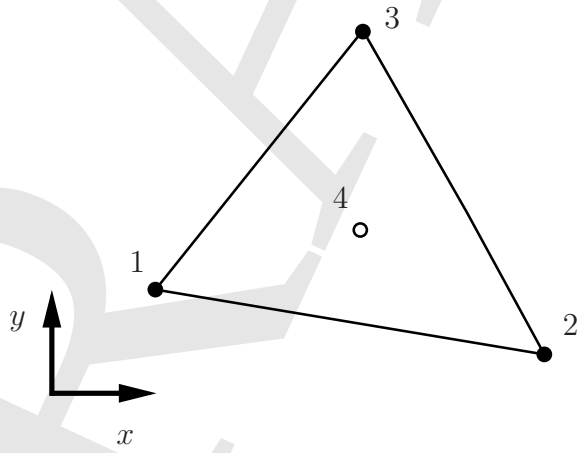

Figure 5.25: *A simple potential 3- or 4-node triangular element for the case* $p = 2$ *(*$u, \dfrac{\partial u}{\partial s}, \dfrac{\partial u}{\partial n}$ *dofs at nodes* $1, 2, 3$ *and, possibly,* u *dof at node* 4*)*

In either case, consider a typical edge, say 1-2, of this element and, without any loss of generality, recast the degrees of freedom associated with this edge relative to the coordinates (s, n), as shown in Figure 5.26. It is clear from the original interpolation assumption that u_h varies cubically in edge 1-2. Hence, given that both u_h and $\dfrac{\partial u_h}{\partial s}$ are specified on this

edge, it follows that u_h, as well as $\dfrac{\partial u_h}{\partial s}$ are continuous across 1-2. However, this is not the case for the normal derivative $\dfrac{\partial u_h}{\partial n}$, which varies quadratically along 1-2, but cannot be determined uniquely from the two normal derivative degrees of freedom on the edge. This implies that $\dfrac{\partial u_h}{\partial n}$ is discontinuous across 1-2, therefore this simple element violates the integrability requirement for the case $p = 2$. Hence, a mere extension of the one-dimensional Hermitian interpolation-based elements to the two-dimensional case is not permissible. To

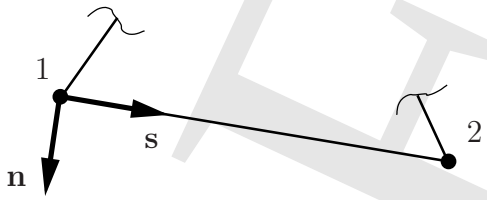

Figure 5.26: *Illustration of violation of the integrability requirement for the 9- or 10-dof triangle for the case* $p = 2$

remedy this problem, one may resort to elements that have mid-edge degrees of freedom, such as the 6-node triangle in Figure 5.27. This element has the previously noted three degrees of freedom at the vertices, as well as a normal derivative degree of freedom at each of the mid-edges.

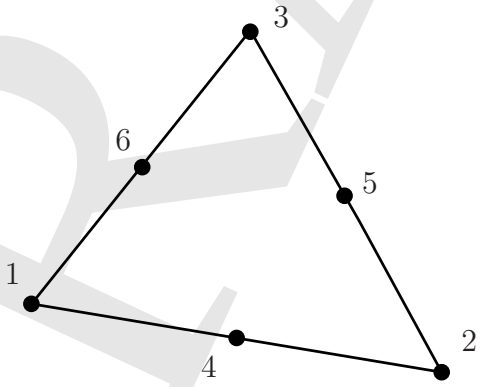

Figure 5.27: *A 12-dof triangular element for the case* $p = 2$ *(*$u, \dfrac{\partial u}{\partial s}, \dfrac{\partial u}{\partial n}$ *dofs at nodes* $1, 2, 3$ *and* $\dfrac{\partial u}{\partial n}$ *at nodes* $4, 5, 6$*)*

The mid-edge nodes of the previous 12-dof element are somewhat undesirable from a data management viewpoint (they have different number of degrees of freedom than vertex

nodes), as well as because of the special care needed in order to specify a unique normal to a given edge (otherwise, the shared degree of freedom would be inconsistently interpreted by the two neighboring elements that share it). More importantly, it turns out that this element requires algebraically complex rational polynomial interpolations for the mid-edge degrees of freedom.

Composite triangles, such as the celebrated Clough-Tocher element, were developed to circumvent the need for rational polynomial interpolation functions. This element is comprised of three joined triangles, each employing a complete cubic interpolation of u_h, see Figure 5.28. This means that, at the outset, the element has $3 \times 10 = 30$ degrees of freedom. Taking into account that the values of u_h and its two first derivatives are shared at each of the four vertices (three exterior and one interior), the total number of degrees of freedom is immediately reduced to 15. At this stage, the normal derivative is not continuous across the internal edges, hence u_h is not internally C^1-continuous. To fix this problem, Clough and Tocher required that the normal derivative be matched at the mid-point of each internal edge, which further reduces the number of degrees of freedom from 15 to 12. These degrees of freedom are u_h, $\dfrac{\partial u_h}{\partial x}$ and $\dfrac{\partial u_h}{\partial y}$ at the corner nodes and $\dfrac{\partial u_h}{\partial n}$ at the mid-edges. In addition, the mid-edge degrees of freedom may be suppressed by requiring that $\dfrac{\partial u_h}{\partial n}$ at the mid-edges be averaged over the two corresponding corner values, thus leading to a 9 degree-of-freedom element. In either case, the Clough-Tocher element possesses piecewise cubic polynomial interpolation of the dependent variable in each triangular subdomain and satisfies both the integrability and the completeness requirement.

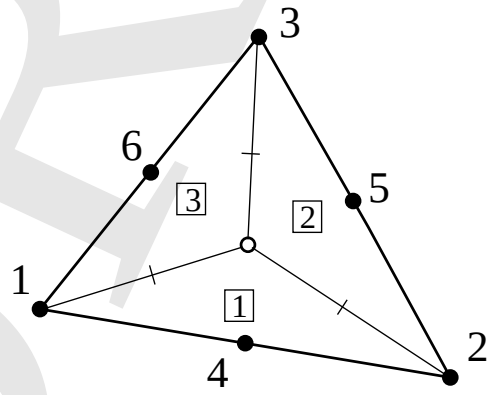

Figure 5.28: *Clough-Tocher triangular element for the case* $p = 2$ *(*$u, \dfrac{\partial u}{\partial s}, \dfrac{\partial u}{\partial n}$ *dofs at nodes* $1, 2, 3$ *and* $\dfrac{\partial u}{\partial n}$ *at nodes* $4, 5, 6$*)*

There are numerous triangular and quadrilateral elements for the case $p = 2$. However, their use has gradually diminished in finite element practice. For this reason, they will not be discussed here in any further detail.

5.5.3 Interpolations in three dimensions

In this section, three dimensional polynomial interpolations are considered in connection with tetrahedral, pentahedral and hexahedral elements.

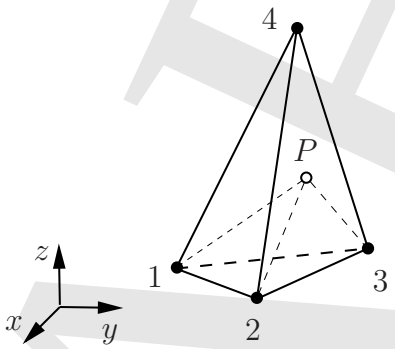

Figure 5.29: *The 4-node tetrahedral element*

The simplest three-dimensional element is the four-node tetrahedron with one node at each vertex, see Figure 5.29. This element has one degree-of-freedom at each node and the dependent variable is interpolated as

$$u_h \;=\; \sum_{i=1}^{4} N_i^e u_i^e \;=\; c_0 + c_1 x + c_2 y + c_3 z \;, \tag{5.86}$$

where u_i^e, $i = 1 - 4$, are the nodal degrees of freedom and $c_0 - c_3$ are constants. Recalling again that $u_i = u_h(x_i^e, y_i^e, z_i^e)$, i.e., that the degrees of freedom take the values of the ordinates of the depended variable at nodes i with coordinates (x_i^e, y_i^e, z_i^e), it follows that the constants $c_0 - c_3$ can be determined by solving the system of equations

$$\begin{aligned}
u_1^e &= c_0 + c_1 x_1^e + c_2 y_1^e + c_3 z_1^e \;, \\
u_2^e &= c_0 + c_1 x_2^e + c_2 y_2^e + c_3 z_2^e \;, \\
u_3^e &= c_0 + c_1 x_3^e + c_2 y_3^e + c_3 z_3^e \;, \\
u_4^e &= c_0 + c_1 x_4^e + c_2 y_4^e + c_3 z_4^e \;.
\end{aligned} \tag{5.87}$$

Clearly, this element is polynomially complete to degree $q = 1$. In addition, it is easy to show that this element is suitable for approximating weak forms in which $p = 1$, i.e., it satisfies the integrability condition for this class of weak forms.

Higher-order tetrahedral elements are possible and, in fact, often used in engineering practice. The next element in this hierarchy is the 10-node tetrahedron with nodes added to each of the six mid-edges. This element is polynomially complete to degree $q = 2$ and can exactly represent any polynomial function consisting of the monomial terms $\{1, x, y, z, x^2, xy, y^2, xy, yz, zx\}$, see Figure 5.30.

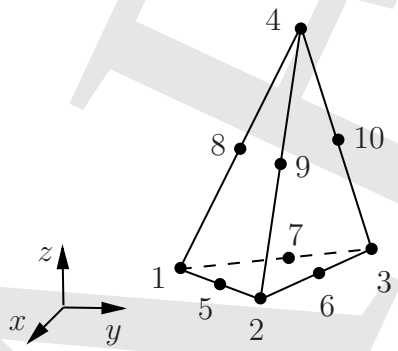

Figure 5.30: *The 10-node tetrahedral element*

The task of deducing analytical representations of the element interpolation functions N_i^e for tetrahedra is vastly simplified by the introduction of *volume coordinates*, in complete analogy to the area coordinates employed for triangular elements in two dimensions. With reference to the 4-node tetrahedral element of Figure 5.30, one may define the volume coordinate L_i of a typical point P in the interior of the tetrahedron as

$$L_i \;=\; \frac{V_i}{V} \quad , \quad i = 1 - 4 \; , \tag{5.88}$$

where V_i is the volume of the tetrahedron formed by the point P and the face opposite to node i, while V is the volume of the full tetrahedron. It is readily obvious that $L_1 + L_2 + L_3 + L_4 = 1$, hence only three of the volume coordinates are independently specified. Also, with reference to the 4-node tetrahedron, it follows that $N_i^e = L_i$, $i = 1 - 4$. Element interpolation functions for higher-order tetrahedra can be derived with great ease using volume coordinates. Furthermore, when evaluating integral terms over tetrahedral regions, one may employ a convenient formula, according to which

$$\int_{\Omega^e} L_1^\alpha L_2^\beta L_3^\gamma L_4^\delta \, dV \;=\; \frac{\alpha!\,\beta!\,\gamma!\,\delta!}{(\alpha \,+\, \beta \,+\, \gamma \,+\delta \,+\, 3)!}\, 6V \; , \tag{5.89}$$

where α, β, γ and δ are integers.

The first two pentahedral elements of interest are the 6-node and the 15-node pentahedron, shown in Figure 5.31. The former is complete up to polynomial degree $q = 1$ and its interpolation functions are capable of representing the monomial terms $\{1, x, y, z, xz, yz\}$. The latter is complete up to polynomial degree $q = 2$ and its interpolation functions may independently reproduce the monomials $\{1, x, y, x^2, xy, y^2, z, xz, yz, x^2z, xyz, y^2z, z^2, xz^2, yz^2\}$. It is worth noting that the interpolation functions of a pentahedral element are products of the triangle-based functions of the top and bottom (triangular) faces and the rectangle-based functions of the lateral (rectangular) faces.

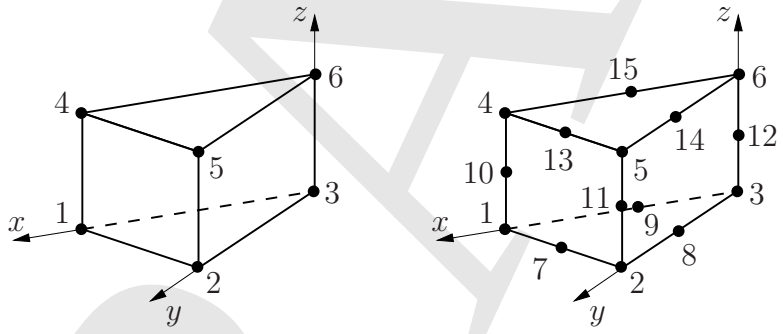

Figure 5.31: *The 6- and 15-node pentahedral elements*

Hexahedral elements are widely used in three-dimensional finite element analyses. The simplest such element is the 8-node hexahedron with nodes at each of its vertices, see Figure 5.32. This element is polynomially complete up to degree $q = 1$ and its interpolation functions are capable of representing any polynomial consisting of $\{1, x, y, z, xy, yz, zx, xyz\}$. The element interpolation functions of the *orthogonal* 8-node hexahedron of Figure 5.32, can

be written by inspection as

$$\begin{aligned}
N_1^e &= -\frac{1}{abc}(x-a)(y-b)(z-c)\ ,\\
N_2^e &= \frac{1}{abc}(x-a)y(z-c)\ ,\\
N_3^e &= -\frac{1}{abc}(x-a)yz\ ,\\
N_4^e &= \frac{1}{abc}(x-a)(y-b)z\ ,\\
N_5^e &= \frac{1}{abc}x(y-b)(z-c)\ ,\\
N_6^e &= -\frac{1}{abc}xy(z-c)\ ,\\
N_7^e &= \frac{1}{abc}xyz\ ,\\
N_8^e &= -\frac{1}{abc}x(y-b)z\ .
\end{aligned} \tag{5.90}$$

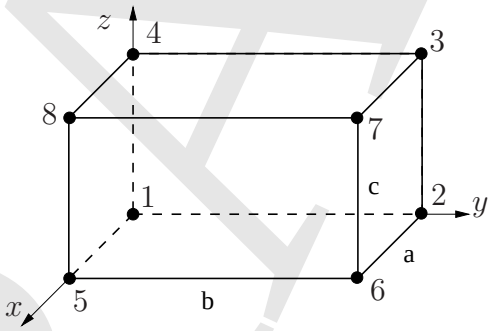

Figure 5.32: *The 8-node hexahedral element*

The next two useful hexahedral elements are the 20- and the 27-node element, see Figure 5.33. These can be viewed as the three-dimensional members of the serendipity and Lagrangian family for the case of polynomial completeness of order $q = 2$. The interpolation functions of the 20-node hexahedron can independently represent the monomials

$$\{1, x, y, z, x^2, y^2, z^2, xy, yz, zx, xyz, xy^2, xz^2, yz^2, yx^2, zx^2, zy^2, x^2yz, y^2zx, z^2xy\}\ ,$$

while the interpolation functions of the 27-node hexahedron can additionally represent the monomials

$$\{x^2y^2, y^2z^2, z^2x^2, x^2y^2z, y^2z^2x, z^2x^2y, x^2y^2z^2\}\ .$$

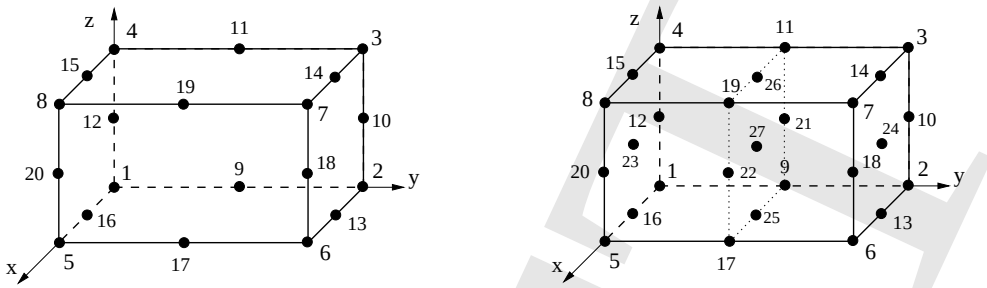

Figure 5.33: *The 20- and 27-node hexahedral elements*

There exist various three-dimensional elements for the case $p = 2$. However, they will not be discussed here owing to their limited usefulness.

5.6 The concept of isoparametric mapping

In finite element practice, one often distinguishes between analyses conducted on *structured* or *unstructured* meshes. The former are applicable to domains that are very regular, such as rectangles, cubes, etc, and which can be subdivided into equal-sized elements, themselves having a regular shape. The latter is encountered in the discretization of complex two- and three-dimensional domains, where it is frequently essential to use elements with "irregular" shapes, such as arbitrary straight-edge quadrilaterals, curved-edge triangles and quadrilaterals, etc. For these cases, it becomes extremely important to establish a general methodology for constructing irregular-shaped elements which satisfy the appropriate completeness and integrability requirements.

The concept of isoparametric mapping offers precisely the means for constructing irregular-shaped elements that inherit the well-established completeness and integrability properties of their regular-shaped counterparts. The main idea of the isoparametric mapping is to construct the irregularly-shaped element in the *physical* domain (i.e., the domain of interest) as a mapping from a *parent* domain in which this same element has a regular shape. This mapping can be expressed in three-dimensions as

$$x \;=\; \hat{x}(\xi,\eta,\zeta) \quad , \quad y \;=\; \hat{y}(\xi,\eta,\zeta) \quad , \quad z \;=\; \hat{z}(\xi,\eta,\zeta)\;, \tag{5.91}$$

where (ξ,η,ζ) and (x,y,z) are coordinates in the natural and physical domain, respectively. The mapping of equations (5.91) can be equivalently (and more succinctly) represented in

vector form as

$$\mathbf{x} \;=\; \boldsymbol{\phi}(\boldsymbol{\xi}) \;, \tag{5.92}$$

where $\mathbf{x} = [x \;\; y \;\; z]^T$ and $\boldsymbol{\xi} = [\xi \;\; \eta \;\; \zeta]^T$. Here, $\boldsymbol{\phi}$ maps the regular-shaped domain $\Omega^e_\square$ to the irregular-shaped domain Ω^e, see Figure 5.34. By way of background, the mapping $\boldsymbol{\phi}$ is termed *one-to-one* (or *injective*) if for any two distinct points $\boldsymbol{\xi}_1 \neq \boldsymbol{\xi}_2$ in $\Omega^e_\square$, their images $\mathbf{x}_1$ and $\mathbf{x}_2$ under $\boldsymbol{\phi}$ satisfy $\mathbf{x}_1 \neq \mathbf{x}_2$. Further, the mapping $\boldsymbol{\phi}$ is termed *onto* (or *surjective*) if $\boldsymbol{\phi}(\Omega^e_\square) = \Omega^e$, or, said equivalently, any point $\mathbf{x} \in \Omega^e$ is the image of some point $\boldsymbol{\xi} \in \Omega^e_\square$.

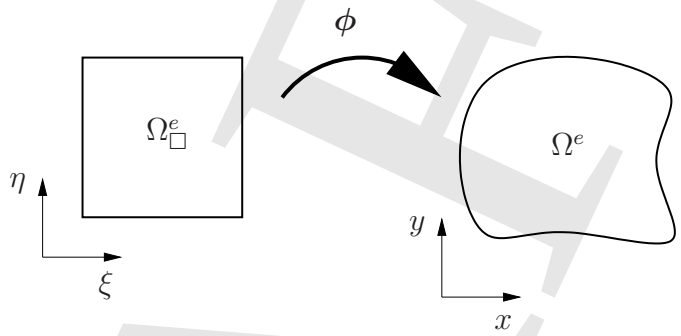

Figure 5.34: *Schematic of a parametric mapping from* $\Omega^e_\square$ *to* Ω^e

In order to define what constitutes an isoparametric mapping, let the dependent variable u be approximated inside the element Ω^e of interest as

$$u^e_h \;=\; \sum_{i=1}^{n} N^e_i u^e_i \;, \tag{5.93}$$

where u^e_i, $i = 1-n$, are the element degrees of freedom. Likewise, suppose that the geometry of the element Ω^e is defined by the equations

$$\mathbf{x} \;=\; \sum_{j=1}^{m} N^e_j \mathbf{x}^e_j \;, \tag{5.94}$$

where $\mathbf{x}^e_j$, $j = 1-m$, are the coordinates of element nodes. It is important to stress that in the preceding equations, the interpolation functions N^e_i and N^e_j are identical for $i = j$ and they are defined on $\Omega^e_\square$, namely they are functions of the natural coordinates (ξ, η, ζ).

With reference to equations (5.93) and (5.94), a finite element is termed *isoparametric* if $n = m$. Otherwise, it is called *subparametric* if $n > m$ or *superparametric* if $n < m$. From the foregoing definition, it follows that in isoparametric elements the same functions are employed to to define the element geometry and the interpolation of the dependent variable. The implications of this assumption will become apparent in the ensuing developments.

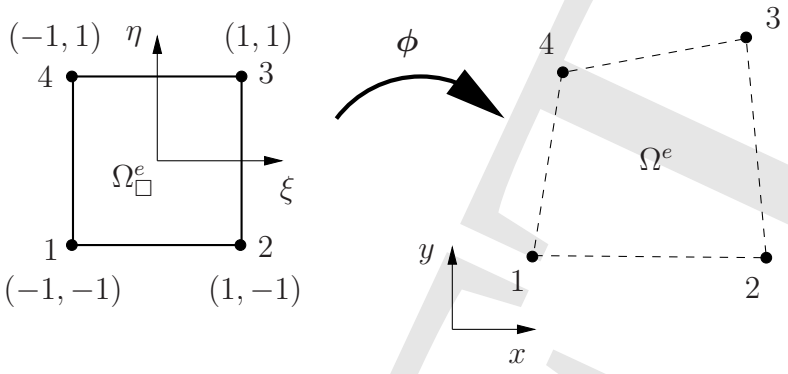

Figure 5.35: *The 4-node isoparametric quadrilateral*

By way of a concrete example, consider in detail the isoparametric 4-node quadrilateral element of Figure 5.35. The element interpolation functions in the parent domain are given by

$$\begin{aligned} N_1^e(\xi,\eta) &= \frac{1}{4}(1-\xi)(1-\eta)\ , \\ N_2^e(\xi,\eta) &= \frac{1}{4}(1+\xi)(1-\eta)\ , \\ N_3^e(\xi,\eta) &= \frac{1}{4}(1+\xi)(1+\eta)\ , \\ N_4^e(\xi,\eta) &= \frac{1}{4}(1-\xi)(1+\eta)\ . \end{aligned} \tag{5.95}$$

Given that the element is isoparametric, it follows that

$$u_h^e = \sum_{i=1}^{4} N_i^e u_i^e \qquad , \qquad \mathbf{x} = \sum_{i=1}^{4} N_i^e \mathbf{x}_i^e\ , \tag{5.96}$$

where $\mathbf{x}_i^e$ are the vectors with coordinates (x_i^e, y_i^e) pointing to the positions of the four nodes $1-4$ in the physical domain.

First, verify that the edges of the element in the physical domain are straight. To this end, consider a typical edge, say 1-2: clearly, this edge corresponds in the parent domain to $\xi \in (-1,1)$ and $\eta = -1$. In view of (5.95) and $(5.96)_2$, this means that the equations describing the edge 1-2 are:

$$\begin{aligned} x &= \frac{1}{2}(1-\xi)x_1^e + \frac{1}{2}(1+\xi)x_2^e = \frac{1}{2}(x_1^e + x_2^e) + \frac{1}{2}\xi(x_2^e - x_1^e)\ , \\ y &= \frac{1}{2}(1-\xi)y_1^e + \frac{1}{2}(1+\xi)y_2^e = \frac{1}{2}(y_1^e + y_2^e) + \frac{1}{2}\xi(y_2^e - y_1^e)\ . \end{aligned} \tag{5.97}$$

The above are parametric equations of a straight line passing through points (x_1^e, y_1^e) and (x_2^e, y_2^e), namely through nodes 1 and 2, which proves the original assertion. Hence, the mapped domain Ω^e is a quadrilateral with straight edges.

Next, establish the completeness and integrability properties of this element. Starting with the former, note that for completeness to polynomial degree $q = 1$, the interpolation of equation $(5.96)_1$ needs to be able to exactly represent any polynomial of the form

$$u_h \;=\; c_0 + c_1 x + c_2 y \;. \tag{5.98}$$

However, equation $(5.96)_1$ implies that, if the four degrees of freedom u_i^e coincide with the nodal values of u_h, then setting u_h at the four nodes according to $(5.96)_1$ yields

$$\begin{aligned} u_h \;&=\; \sum_{i=1}^{4} N_i^e u_i^e \;=\; \sum_{i=1}^{4} N_i^e u_h(x_i^e, y_i^e) \;=\; \sum_{i=1}^{4} N_i^e (c_0 + c_1 x_i^e + c_2 y_i^e) \\ &=\; (\sum_{i=1}^{4} N_i^e) c_0 + (\sum_{i=1}^{4} N_i^e x_i^e) c_1 + (\sum_{i=1}^{4} N_i^e y_i^e) c_2 \;=\; (\sum_{i=1}^{4} N_i^e) c_0 + c_1 x + c_2 y \;, \end{aligned} \tag{5.99}$$

where equation $(5.96)_2$ is used. In view of equation (5.98), completeness of the 4-node isoparametric quadrilateral is guaranteed as long as $\sum_{i=1}^4 N_i^e = 1$, which can be easily verified from equations (5.95).

Integrability for the case $p = 1$ can be established as follows: consider a typical element edge, say 1-2, along which

$$u_h(\xi, -1) \;=\; \frac{1}{2}(1-\xi) u_1^e + \frac{1}{2}(1+\xi) u_2^e \;, \tag{5.100}$$

as readily seen from equations (5.95) and $(5.96)_1$. The preceding expression confirms that the value of u_h along edge 1-2 is a linear function of the variable ξ and depends solely on the nodal values of u_h at nodes 1 and 2. This, in turn, implies continuity of u_h across the edge 1-2, which is a sufficient condition for integrability.

One of the key questions associated with isoparametric finite elements is whether the isoparametric mapping $\boldsymbol{\phi}$, expressed here through equations $(5.96)_2$, is invertible. Said differently, the relevant question is whether one may uniquely associate points $(\xi, \eta) \in \Omega^e_\square$ with points $(x, y) \in \Omega^e$ and vice-versa. This question is addressed by the *inverse function theorem*, which, when adapted to the context of this problem may be stated as follows: Consider a mapping $\boldsymbol{\phi} : \Omega^e_\square \mapsto \Omega^e$ of class C^r, such that $\boldsymbol{\xi} \in \Omega^e_\square$ is mapped to $\mathbf{x} = \boldsymbol{\phi}(\boldsymbol{\xi}) \in \Omega^e$, where $\Omega^e_\square$ and Ω^e are open sets. If $J = \det \dfrac{\partial \boldsymbol{\phi}}{\partial \boldsymbol{\xi}} \neq 0$ at a point $\bar{\boldsymbol{\xi}} \in \Omega^e_\square$, then there is an open

neighborhood around $\boldsymbol{\xi}$, such that $\boldsymbol{\phi}$ is one-to-one and onto an open subset of Ω^e containing the point $\bar{\mathbf{x}} = \boldsymbol{\phi}(\bar{\boldsymbol{\xi}})$ and the inverse function $\boldsymbol{\phi}^{-1}$ exists and is of class C^r.

The derivative $\mathbf{J} = \dfrac{\partial \boldsymbol{\phi}}{\partial \boldsymbol{\xi}}$ can be written in matrix form as

$$[J] \;=\; \begin{bmatrix} \dfrac{\partial \hat{x}}{\partial \xi} & \dfrac{\partial \hat{x}}{\partial \eta} \\ \dfrac{\partial \hat{y}}{\partial \xi} & \dfrac{\partial \hat{y}}{\partial \eta} \end{bmatrix}, \tag{5.101}$$

and is referred to as the *Jacobian matrix* of the isoparametric transformation. The inverse function theorem guarantees that every interior point $(x, y) \in \Omega^e$ is uniquely associated with a single point $(\xi, \eta) \in \Omega^e_\square$ provided that the determinant J is non-zero everywhere in $\Omega^e_\square$.[3]

Given equation (5.101), the Jacobian determinant J is given by

$$J \;=\; \frac{\partial \hat{x}}{\partial \xi}\frac{\partial \hat{y}}{\partial \eta} - \frac{\partial \hat{y}}{\partial \xi}\frac{\partial \hat{x}}{\partial \eta}\,, \tag{5.102}$$

which, taking into account equation $(5.96)_2$, leads, after some elementary algebra, to

$$\begin{aligned} J \;=\; \frac{1}{8}\big[&(x_1^e y_2^e - x_2^e y_1^e + x_2^e y_3^e - x_3^e y_2^e + x_3^e y_4^e - x_4^e y_3^e + x_4^e y_1^e - x_1^e y_4^e) \\ &+ \xi(x_1^e y_4^e - x_4^e y_1^e + x_2^e y_3^e - x_3^e y_2^e + x_3^e y_1^e - x_1^e y_3^e + x_4^e y_2^e - x_2^e y_4^e) \\ &+ \eta(x_1^e y_3^e - x_3^e y_1^e + x_2^e y_1^e - x_1^e y_2^e + x_3^e y_4^e - x_4^e y_3^e + x_4^e y_2^e - x_2^e y_4^e)\big]\,. \end{aligned} \tag{5.103}$$

It is instructive to observe here that since J is linear in ξ and η, then $J > 0$ everywhere in

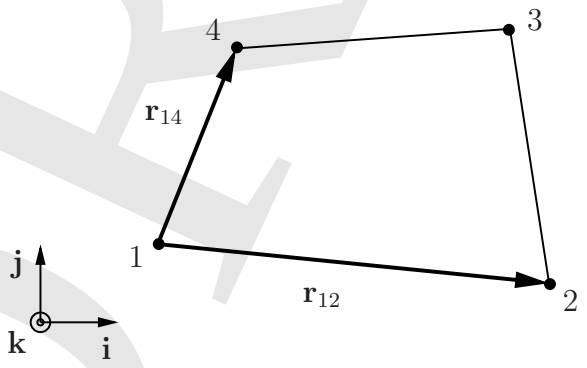

Figure 5.36: *Geometric interpretation of one-to-one isoparametric mapping in the 4-node quadrilateral*

[3] Note that here $\boldsymbol{\phi}$ is of class C^∞.

the interior of the domain $\Omega^e_\square$ if $J > 0$ at all four nodal points. Now, consider node 1, with natural coordinates $(-1, -1)$ and conclude from equation (5.103) that at this node

$$J(-1,-1) \;=\; \frac{1}{4}\big[(x_2^e - x_1^e)(y_4^e - y_1^e) - (x_4^e - x_1^e)(y_2^e - y_1^e)\big] \;. \tag{5.104}$$

It follows from the above equation that $J > 0$ if the physical domain Ω^e is convex at node 1. This is because, with reference to Figure 5.36, one may interpret the Jacobian determinant at node 1 according to

$$4J\mathbf{k} \;=\; \mathbf{r}_{12} \times \mathbf{r}_{14} \;, \tag{5.105}$$

where $\mathbf{r}_{ij}$ denotes the vector connecting nodes i and j and $\mathbf{k}$ is the unit vector normal to the plane of the element, such that $(\mathbf{r}_{12}, \mathbf{r}_{14}, \mathbf{k})$ form a right-handed triad. An analogous conclusion can be drawn for the other three nodes. Hence, invertibility of the isoparametric mapping for the 4-node quadrilateral is guaranteed as long as the element domain Ω^e is convex, see Figure 5.37.

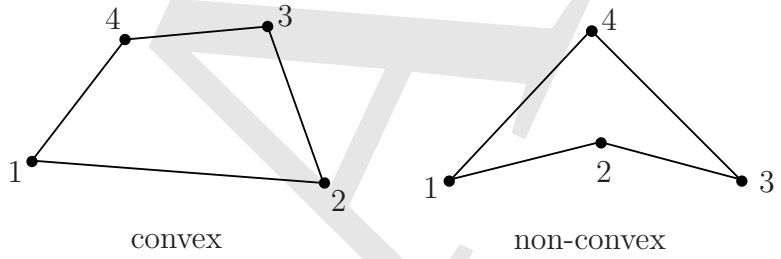

Figure 5.37: *Convex and non-convex 4-node quadrilateral element domains*

It is easy to see that the isoparametric mapping in Figure 5.35 is orientation-preserving, in the sense that the nodal sequencing (say 1-2-3-4, if following a counter-clockwise convention) is preserved under the mapping $\boldsymbol{\phi}$. While this orientation preservation property is not essential, it is typically adopted in finite element practice. Reversal of the node sequencing, say from (1-2-3-4) to (1-4-3-2) when following a counterclockwise convention implies that $J < 0$. This can be immediately seen using the foregoing interpretation of the Jacobian determinant at nodal points.

An additional property of the Jacobian determinant J, which becomes important when evaluating integrals associated with weak forms, is deduced for the 4-node quadrilateral. To this end, note that

$$dx \;=\; \frac{\partial \hat{x}}{\partial \xi} d\xi + \frac{\partial \hat{x}}{\partial \eta} d\eta \qquad , \qquad dy \;=\; \frac{\partial \hat{y}}{\partial \xi} d\xi + \frac{\partial \hat{y}}{\partial \eta} d\eta \;. \tag{5.106}$$

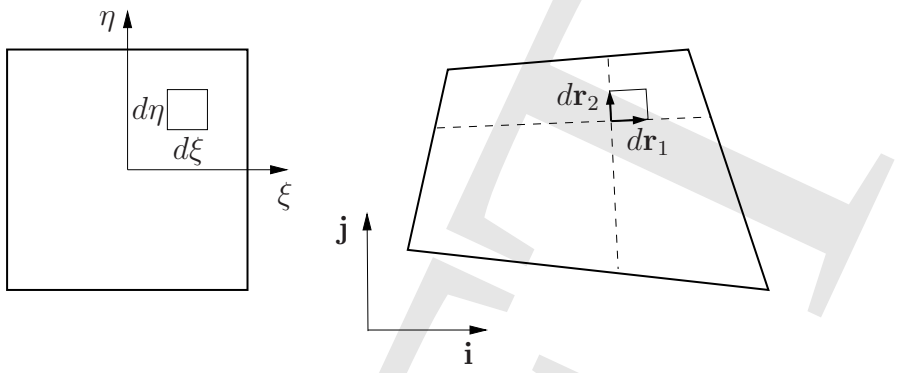

Figure 5.38: *Relation between area elements in the natural and physical domain*

Hence, with reference to Figure 5.38, the infinitesimal vector area $d\mathbf{A}$ is written as

$$d\mathbf{A} \;=\; d\mathbf{r}_1 \times d\mathbf{r}_2 \;, \tag{5.107}$$

where $d\mathbf{r}_1$ and $d\mathbf{r}_2$ are the infinitesimal vectors along lines of constant η and ξ, respectively. This implies that

$$d\mathbf{A} \;=\; (\frac{\partial \hat{x}}{\partial \xi} d\xi \mathbf{i} + \frac{\partial \hat{y}}{\partial \xi} d\xi \mathbf{j}) \times (\frac{\partial \hat{x}}{\partial \eta} d\eta \mathbf{i} + \frac{\partial \hat{y}}{\partial \eta} d\eta \mathbf{j}) \;=\; J d\xi d\eta \mathbf{k} \;, \tag{5.108}$$

where $(\mathbf{i}, \mathbf{j})$ are unit vectors along the x- and y-axis, respectively. It follows from the above equation that the infinitesimal area element dA in the physical domain is related to the infinitesimal area element $d\xi d\eta$ in the natural domain as

$$dA \;=\; J d\xi d\eta \;. \tag{5.109}$$

The above argument has not made specific use of the isoparametric mapping of the 4-node quadrilateral element, hence it applies to all planar isoparametric elements. This argument can be easily extended to three-dimensional elements or restricted to one-dimensional elements of the isoparametric type.

The isoparametric approach can be applied to triangles and quadrilaterals without appreciable complication over what has been described for the 4-node quadrilateral. For example, higher-order planar isoparametric elements can be constructed based on the 6-node triangle and the 8-node serendipity rectangle, see Figure 5.39. Both elements may have curved boundaries, which is a desirable feature when modeling arbitrary domains.

Three-dimensional isoparametric elements are also possible and, in fact, quite popular. The simplest such element is the 8-node isoparametric brick of Figure 5.40. The geometry

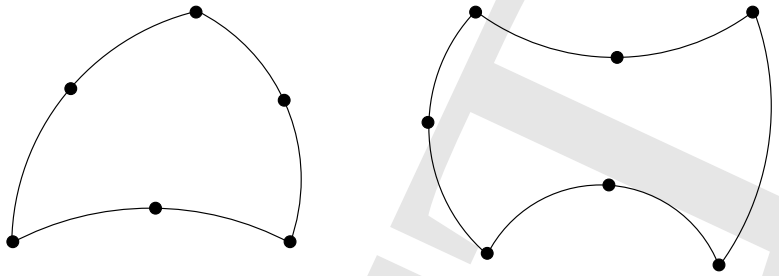

Figure 5.39: *Isoparametric 6-node triangle and 8-node quadrilateral*

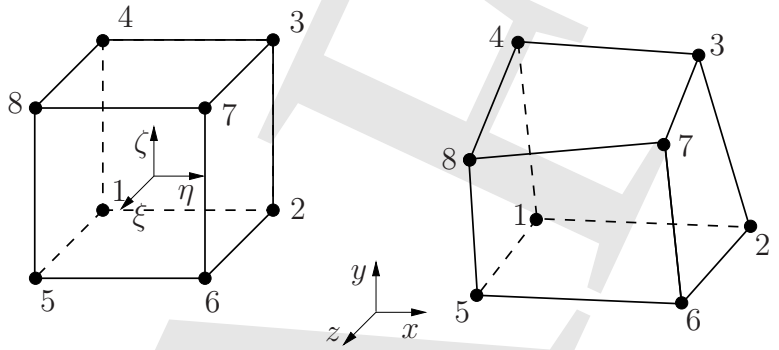

Figure 5.40: *Isoparametric 8-node hexahedral element*

of this element is defined in terms of the position vectors $\mathbf{x}_i$ of its eight vertex nodes and the corresponding interpolation functions N_i^e in the natural domain. The latter can be written relative to the coordinate system shown in Figure 5.40 as

$$\begin{aligned}
N_1^e &= \frac{1}{4}(1-\xi)(1-\eta)(1-\zeta) \quad , \quad N_2^e = \frac{1}{4}(1-\xi)(1+\eta)(1-\zeta) \ , \\
N_3^e &= \frac{1}{4}(1-\xi)(1+\eta)(1+\zeta) \quad , \quad N_4^e = \frac{1}{4}(1-\xi)(1-\eta)(1+\zeta) \ , \\
N_5^e &= \frac{1}{4}(1+\xi)(1-\eta)(1-\zeta) \quad , \quad N_6^e = \frac{1}{4}(1+\xi)(1+\eta)(1-\zeta) \ , \\
N_7^e &= \frac{1}{4}(1+\xi)(1+\eta)(1+\zeta) \quad , \quad N_8^e = \frac{1}{4}(1+\xi)(1-\eta)(1+\zeta) \ .
\end{aligned} \tag{5.110}$$

All element edges in the 8-node isoparametric brick are straight. Indeed, a typical edge, say 8-7 with coordinates $(1, \eta, 1)$, is described by the equations

$$\begin{aligned}
x &= \frac{1}{2}(x_7^e + x_8^e) + \frac{1}{2}(x_7^e - x_8^e)\eta \ , \\
y &= \frac{1}{2}(y_7^e + y_8^e) + \frac{1}{2}(y_7^e - y_8^e)\eta \ , \\
z &= \frac{1}{2}(z_7^e + z_8^e) + \frac{1}{2}(z_7^e - z_8^e)\eta \ ,
\end{aligned} \tag{5.111}$$

which are precisely the parametric equations of a straight line passing through the nodal points 7 and 8 with coordinates (x_7^e, y_7^e, z_7^e) and (x_8^e, y_8^e, z_8^e), respectively. However, element faces are not necessarily flat. To argue this point, take a typical face, say 8-7-4-3 with coordinates $(\xi, \eta, 1)$ and note that it is defined by the equations

$$\begin{aligned} x &= \frac{1}{4}(1-\xi)(1+\eta)x_3^e + \frac{1}{4}(1-\xi)(1-\eta)x_4^e + \frac{1}{4}(1+\xi)(1+\eta)x_7^e + \frac{1}{4}(1+\xi)(1-\eta)x_8^e \ , \\ y &= \frac{1}{4}(1-\xi)(1+\eta)y_3^e + \frac{1}{4}(1-\xi)(1-\eta)y_4^e + \frac{1}{4}(1+\xi)(1+\eta)y_7^e + \frac{1}{4}(1+\xi)(1-\eta)y_8^e \ , \\ x &= \frac{1}{4}(1-\xi)(1+\eta)z_3^e + \frac{1}{4}(1-\xi)(1-\eta)z_4^e + \frac{1}{4}(1+\xi)(1+\eta)z_7^e + \frac{1}{4}(1+\xi)(1-\eta)z_8^e \ , \end{aligned} \tag{5.112}$$

which contain a bilinear term $\xi\eta$ responsible for the non-flatness of the resulting surface.[4] As in the case of planar elements, it is straightforward to formulate higher-order three-dimensional isoparametric elements based, e.g., on the 10-node tetrahedron or the 20-node brick. In general, these higher-order elements have both curved edges and non-flat faces.

5.7 Exercises

Problem 1
Write the shape functions for a complete and integrable ($p = 1$) cubic one-dimensional element using standard and hierarchical interpolation.

Problem 2
Write the shape functions for a 10-node triangular element using area coordinates.

Problem 3
Find the shape functions for the following elements of square domain as in the adjacent figure:

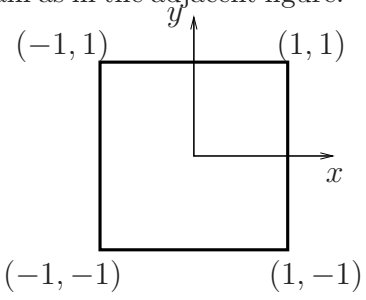

(a) the 8- and 12-node members of the serendipity family,

(b) the 9- and 16-node members of the Lagrangian family,

(c) the hierarchically interpolated 4-node quadratic element corresponding to the 9-node member of the Lagrangian family.

[4] Another way of arguing the same point is to simply note that the element edge needs to pass through 4 points which do not necessarily lie on the same plane.

Problem 4

Consider a non-rectangular 4-node quadrilateral element with standard polynomial shape functions. Give an example showing that in this element the values of the dependent variable along an edge generally depend not only on its values at the two nodes defining the edge, but also on its values at one or both of the other nodes. This observation verifies that the arbitrarily-shaped 4-node quadrilateral typically yields incompatible polynomial finite element approximations for problems with $p = 1$.

Hint: to avoid lengthy calculations, consider a simple non-rectangular element shape for your analysis.

Problem 5

A finite element analysis is performed with rectangular serendipity elements. At a certain location in the domain, the mesh pattern of the figure is desired. Which restriction should be imposed on the nodal values of the dependent variable u_h, so as to maintain compatibility of the admissible field $\mathcal{U}$ for problems with $p = 1$? State precisely the required condition.

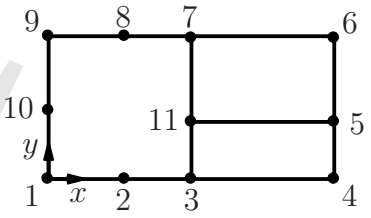

Problem 6

Consider the boundary-value problem of *Problem 2* in Chapter 3, which is to be solved for $k = 1$ and $f = 0$ by a Bubnov-Galerkin approximation. The domain Ω is discretized using finite elements with rectangular domains Ω_e, such that in each element $u_h(\Omega_e) = \sum_i N_i^e u_i^e$ and $w_h(\Omega_e) = \sum_i N_i^e w_i^e$. Subsequently, the weak form of the problem is written for a typical element as

$$\sum_i w_i^e \Big(\sum_j K_{ij}^e u_j^e \; - \; F_i^e \Big) \; = \; 0 \; ,$$

where $\mathbf{K}^e = (K_{ij}^e)$ is the element stiffness matrix and $\mathbf{F}^e = (F_i^e)$ is the forcing vector due to the non-vanishing Neumann boundary conditions on $\partial\Omega_e$.

(a) Derive general formulae for $\mathbf{K}^e$ and $\mathbf{F}^e$ for an element with domain Ω_e, in terms of the element interpolation functions N_i^e.

(b) For the element depicted in the adjacent figure, assume that only the edge with equation $x_1 = 1$ possesses non-zero Neumann boundary conditions and determine specific expressions for $\mathbf{F}_q^e$, provided that the interpolation functions in Ω_e are based on (a) 4-node rectangular, (b) 8-node serendipity, or (c) 9-node Lagrangian elements. In the above analysis, let $\bar{q} = q_0$, where q_0 is a constant, and $\bar{q} = \frac{1}{2}(1-x_2)q_1 + \frac{1}{2}(1+x_2)q_2$, where q_1 and q_2 are constants.

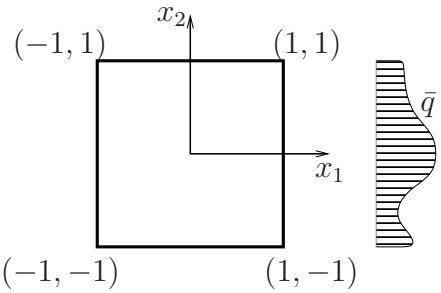

Problem 7

To illustrate a general procedure for the determination of shape functions in rectangular elements, consider the 6-node element in the adjacent figure. First, write the standard bi-linear shape functions for the 4-node element (i.e., ignore, for a moment, the presence of nodes 5 and 6). Subsequently, ignoring only the presence of node 6, write the shape function for node 5 and use it to selectively modify the shape functions for nodes 1 through 4, so as to satisfy all relevant requirements for all five shape functions. Then, repeat this procedure to determine the shape functions of the full 6-node element.

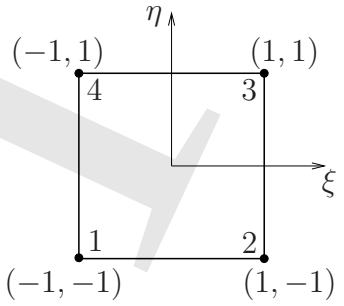

Problem 2

Determine the isoparametric transformation equations and the Jacobian matrix for the element shown in the adjacent figure. Use the standard square parent element $\Omega^e_\square = \{(\xi, \eta) \in (-1, 1) \times (-1, 1)\}$ for the isoparametric transformation.

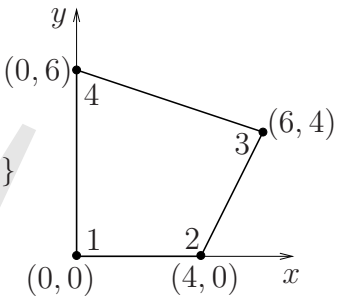

Problem 3

Consider the 8-node isoparametric element of the adjacent figure. Assuming that the location of nodes 1-5 and 7-8 is fixed, determine the extent to which node 6 can move vertically away from the mid-edge point without rendering the mapping from the parent to the actual element singular.

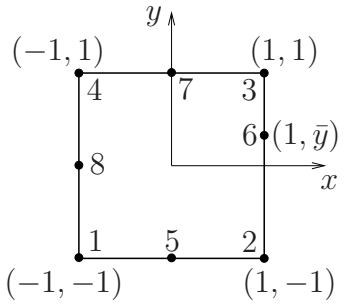

Problem 4

Write the interpolation functions N^e_i, $I = 1 - 15$, for the 15-node triangle using area coordinates. Also, compute the integral $\int_{\Omega^e} N_1 N_6 \, dA$ over the region Ω_e of an equilateral triangle with unit side. What is the degree of polynomial completeness of this element?

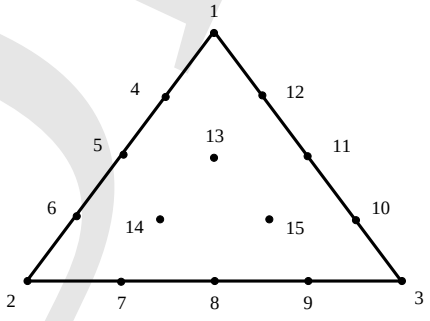

Problem 5

A 3-node triangular element is constructed from a 4-node isoparametric quadrilateral element by collapsing two neighboring nodes to a single point, as shown in the following figure:

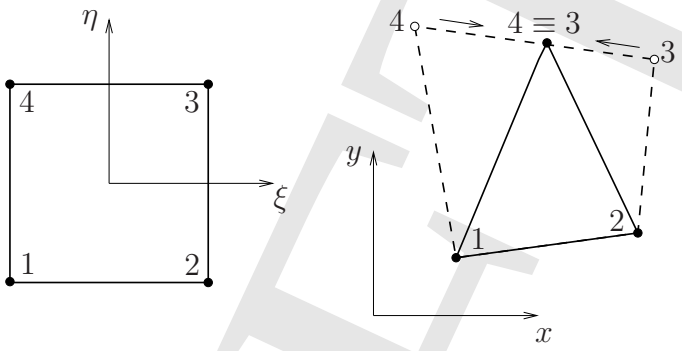

Using a formal procedure, show that the field $u_h = \sum_{I=1}^{4} N_I^e u_I^e$ associated with the above degenerate quadrilateral element is identical to the (linear) field of a standard 3-node triangular element. What can you conclude about the isoparametric transformation at node $3 \equiv 4$?

Hint: Let $(\bar{\xi}, \bar{\eta})$ be the natural coordinates associated with an arbitrary interior point of the above degenerate triangular element. Show that at this point the gradient of $u_h(x, y)$ is independent of $(\bar{\xi}, \bar{\eta})$.